Universidade de Aveiro Departamento de Electrónica, Telecomunicações e Informática,
2017

Gonçalo Nuno
Duarte de Melo Rosa

Sistema de Medida para Fornos Micro-ondas

Measuring System for Microwave Ovens

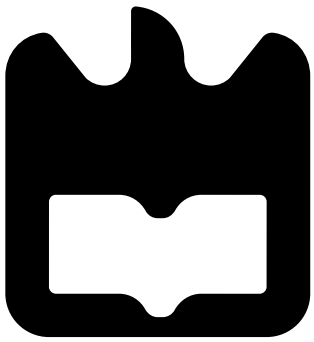

Gonçalo Nuno Duarte de Melo Rosa

Sistema de Medida para Fornos Micro-ondas

Measuring System for Microwave Ovens

Dissertação apresentada à Universidade de Aveiro para cumprimento dos requisitos necessários à obtenção do grau de Mestre em Engenharia Eletrónica e Telecomunicações, realizada sob a orientação científica de Professor Doutor Nuno Miguel Gonçalves Borges de Carvalho, Professor do Departamento de Eletrónica, Telecomunicações e Informática da Universidade de Aveiro.

Dissertation presented to the University of Aveiro for the fulfilment of the necessary requisites to obtain the degree of Master in Electronic and Telecommunications Engineering, developed under the scientific guidance of Professor Nuno Miguel Gonçalves Borges de Carvalho, Professor in the Department of Electronic, Telecommunications and Informatic of the University of Aveiro.

"Imagination is more important than knowledge.
For knowledge is limited to all we now know and understand, while imagination embraces the entire world and all there ever will be to know and understand."

— Albert Einstein

o júri / the jury

presidente / president

Professor Doutor Armando Carlos Domingues da Rocha
Professor Auxiliar da Universidade de Aveiro

vogais / examiners committee

Professor Doutor Rafael Ferreira da Silva Caldeirinha
Professor Coordenador da Escola Superior de Tecnologia e Gestão do Instituto Politécnico de Leiria (arguente)

Professor Doutor Nuno Miguel Gonçalves Borges de Carvalho
Professor Catedrático da Universidade de Aveiro (orientador)

agradecimentos / acknowledgements

Queria começar por agradecer a todos os que contribuíram de forma positiva para os últimos 5 anos e que fizeram deste meu percurso académico digno de relembrar no futuro.

Em especial aos meus pais, que se esforçam todos os dias para que eu consiga seguir os meus sonhos e pelo conselho e apoio que dão.

Um abraço ao meu irmão por tudo o que me ensinou e continua a ensinar.

A dois dos três artolas que desde o primeiro ano estudam, brincam, jogam, têm fé e vivem em conjunto comigo, o João Milheiro e o Ricardo Loureiro, um abraço grande!

Aos colegas do IT de Aveiro e do DETI pela camaradagem e entreajuda, em especial à Mariana Oliveira e à Joana Pereira por me terem ajudado sempre que me foram surgindo dúvidas e questões existenciais.

Um agradecimento ao meu orientador, professor doutor Nuno Borges de Carvalho, pela ajuda e inspiração, ao Paulo Gonçalves, pela imensa ajuda na assemblagem e impressão de todos os circuitos e estruturas, ao Ricardo Correia, Pedro Pinho, Diogo Barros, Andreia Costa e Daniel Belo por toda a ajuda e ensinamentos que me deram durante o desenvolvimento desta dissertação. Queria também agradecer à Ampleon pelo fornecimento dos transístores usados na implementação do conversor de RF para DC.

Ao Pedro Abreu, aos Conde, Ascorujas e a todos os amigos que me apoiaram, duma maneira ou de outra, muitos abraços e beijos. Em especial, ao Hugo que me convenceu a praticar voleibol e deixar de ser preguiçoso.

Para finalizar um obrigado à Layla que entrou na minha vida de repente e apesar de não parar quieta e ser uma medricas é uma boa companhia e, segundo uns, mais inteligente que alguns humanos.

Palavras-Chave Culinária de RF, Forno Micro-ondas, Conversão de RF para DC, Monitorização de Campos Eletromagnéticos, Antena Eletricamente Pequena, Magnetron, Culinária de Estado Sólido, ADS, CST, SolidWorks

Resumo Fornos micro-ondas estão presentes nas nossas vidas desde que Percy Spencer descobriu um chocolate derretido no bolso depois de passar à frente de um magnetron. No entanto, já há mais de 50 anos que eles estão no mercado, a vasta maioria da população tem um em casa e a tecnologia pouco mudou desde então. Várias funcionalidades têm sido desenvolvidas para tentar melhorar e diversificar a maneira como os fornos micro-ondas aquecem a comida, bem como, outras tecnologias para tentar facilitar a observação do interior da cavidade, por exemplo visão infravermelho, auxiliares visuais e simulações eletromagnéticas. Apesar disto, o aquecimento não é feito da melhor forma e a base tecnológica da fonte de energia que aquece a comida não teve nenhum desenvolvimento significativo. Mais recentemente, a área de engenharia de rádio frequência tem desenvolvido imensas aplicações com tecnologias de estado sólido e estão a surgir novos fornos que dispensam o magnetron e conseguem variar a frequência para se adaptarem e aquecerem melhor cada alimento. No entanto, continua a não haver uma ponta de prova que monitorize o campo eletromagnético dentro do forno micro-ondas. Esta dissertação propõe o desenvolvimento de um sistema que monitorize as radiações dentro de um micro-ondas caracterizando-o de um modo mais preciso e com um conjunto de informações muito mais relevantes.

Keywords RF cooking, Microwave Oven, RF to DC Conversion, EMF Monitoring, Electrically Small Antenna, Magnetron, Solid State Cooking, ADS, CST, SolidWorks

Abstract Microwave ovens have been in our lives ever since Percy Spencer noticed his chocolate melting in his pocket after passing in front of a radiating magnetron. However, they have been in the market for more than 50 years, the majority of the population owns one at home and the technology hasn't changed much. Several features have been developed to try to improve and diversify the way microwave ovens heat food, as well as, other technologies to try and make the observation of the interior cavity easier, for instance, infrared (thermal) vision, visual aids and electromagnetic simulation. Even though all that, the heating is not done in the finest way and the technological basis of the energy source that heats food hasn't had any significant development. More recently, the Radio Frequency (RF) engineering field has been developing numerous applications with solid state technology and new ovens are emerging. These devices don't need the magnetron and can vary in frequency to adapt and better heat each food. However, a probe to monitor the electromagnetic field inside the microwave oven still doesn't exist, therefore, this dissertation proposes the development of a system that monitors this radiation, characterising it in a more precise manner together with a set of much more relevant information.

Contents

List of Figures

List of Tables

Acronyms

ADS	Advanced System Design
ANSI	American National Standards Institute
ARPANSA	Australian Radiation Protection and Nuclear Safety Agency
CPW	Coplanar Waveguide
CSRR	Complementary Split Ring Resonator
CST	Computer Simulation Technology
DC	Direct Current
DGS	Defected Ground Structure
DNG	Double Negative
EBG	Electromagnetic Band Gap
FNBW	First-Null Beamwidth
GPS	Global Positioning System
HB	Harmonic Balance
HPBW	Half-Power Beamwidth
ICNIRP	International Commission on Non-Ionizing Radiation Protection
IEC	International Electrotechnical Commission
IMPI	International Microwave Power Institute
IoT	Internet of Things
LSSP	Large Signal S Parameter

NIR	Negative Index of Refraction
PCB	Printed Circuit Board
pHEMT	Pseudomorphic High Electron Mobility Transistor
PIFA	Planar Inverted F Antenna
RF	Radio Frequency
RFID	Radio Frequency Identification
SAR	Specific Absorption Rate
SFF	Small Form Factor
SMA	SubMiniature version A
SPS	Solar Powered Satellites
UHF	Ultra High Frequency
VSG	Vector Signal Generator
WPT	Wireless Power Transmission

Chapter 1

Introduction

1.1 Context and Objectives

Right after the World War II, radar technologies were widely used for radar transmitters which used a magnetron as a power source. Percy Spencer, who worked with high power generators, noticed that he had a melted chocolate bar inside his pocket, due to the microwave radiation generated by a magnetron, [1]. He then tested with other foods before concluding that his snack had granted him the title of the man who discovered the heating capabilities of microwaves. All this happened around 1945, but the first microwave oven was too big (the size of a refrigerator) and used water-cooling to refrigerate the magnetron. It wasn't until 1967, that a microwave oven, with reasonable size and weight, was released into the market, making it the first with a more similar size to those still used nowadays. However, "Since the mid-1970s there has been little change to the basic design of the cooker", [1].

The magnetron power source generates RF energy at a certain bandwidth and frequency (2.45 GHz for those used in microwave ovens) and the only way to change the resonant frequency is by physically changing it. All foodstuffs have their own dielectric and resonant frequency, which means heating them at the frequency that induces a better absorption of microwaves would be ideal. Another aspect the magnetron can't control is the standing wave pattern that produces hotter areas and colder zones that lead to unevenly heated food. The food companies are aware of these deficiencies, and because they can't fix the oven's design, they compensate with ingenious packaging technology, [2], timers and infrared grills to brown food, [1], among other technologies.

This dissertation proposes a system to answer researchers needs, like those of Kerry Parker and Michael Vollmer, [1], who said "It would be wonderful if ovens could be designed to produce an even intensity of microwaves throughout the oven, but unfortunately this is very difficult". This dissertation can also help change the specifications of microwave ovens, which nowadays are standardized "on their ability to heat one litre of water, which presents a large load to the system and is very easy to heat. Standards and specifications drive the performance optimisation process, which leads to products that are optimised for heating a load that will rarely be encountered in real world usage", [3].

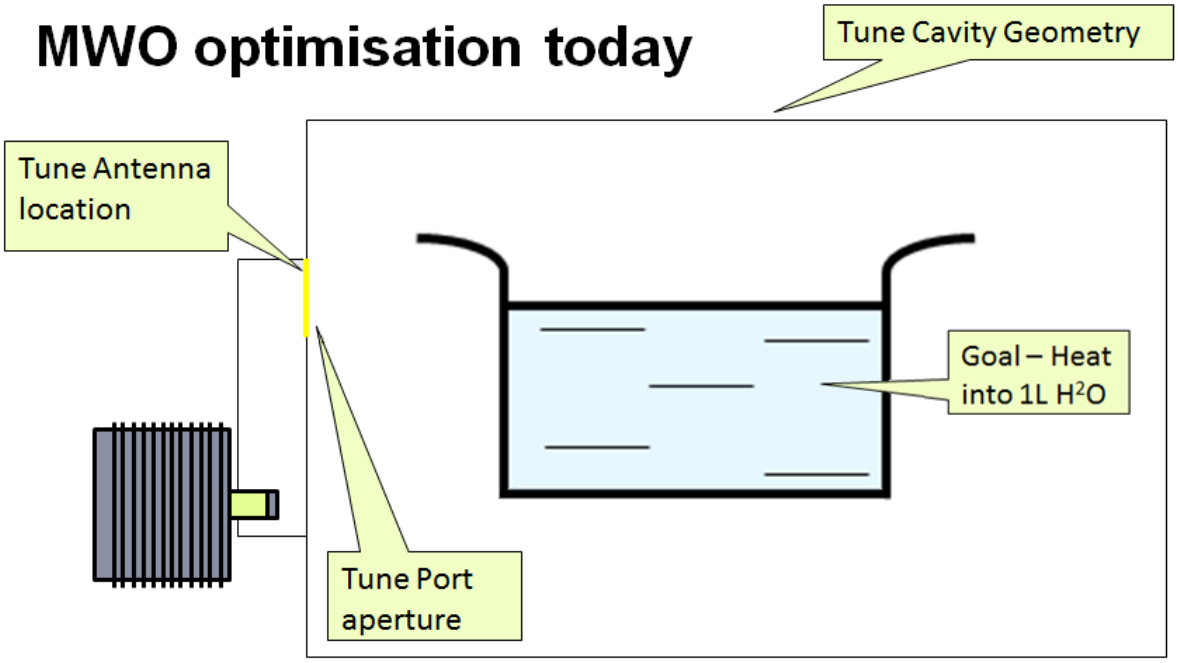

Figure 1.1: Adapted from "Tuning of a Microwave Oven", [3].

The current microwave oven optimisation, as represented in figure 1.1, "has little to do with the magnetron itself", [3], but, since the radiation power generated by the magnetron interacts with the electromagnetic field that is formed inside the resonant cavity, this optimisation is not going to be very accurate. This dissertation proposes a probe, that monitors the electromagnetic field inside the cavity. This would facilitate the optimisation by returning information much more relevant than that from a heated recipient of water, and promote optimisation procedures, in order "to deliever the full promise", [3].

This standard doesn't take frequency of operation into account, i.e. a well performing microwave is considered so when the 1 litre of water is heated regardless of the frequency the magnetron is operating at. New solid state technologies are starting to handle power levels comparable to the magnetron's output power, [3]. Solid state technology also offers a much better control capability in terms of frequency, power, phase and other characteristics in order to deliver the best possible performance. This new technology is revolutionising RF cooking for its ability to integrate heating algorithms, frequency and power adjustment to each and every food. However, apart from measuring the cavity's reflection coefficient, this new technology can't 'see' what is going on inside the microwave oven and could use a measuring probe for easier and faster development.

The proposed measuring probe is based on the design of a rectenna element. This energy-harvesting configuration is mainly used by two scientific communities, Solar Powered Satellites (SPS) and Radio Frequency Identification (RFID). The first is more related to the scope of this dissertation, since RFID applications work with low power signals. The rectenna consists of two parts, the rectifying circuit and the antenna. Since the purpose of this dissertation is to insert a large array of antennas inside the microwave oven, these should be as small as possible. With that in mind, electrically small antenna configurations and metamaterial-inspired techniques are a good approach to miniaturising the antenna.

1.2 Dissertation's Layout

This dissertation's structure will begin with the Introduction and the final chapters will contain the conclusions, future work and bibliography. Apart from these chapters, the dissertation is composed of three other chapters, which are Chapter 2: The Inside and Outside of the Microwave Oven, Chapter 3: Field Detector Probe, and finally Chapter 4: Simulation and Measurement.

Chapter 2 addresses the technologies around the microwave oven. Those that help researchers and enthusiasts have a notion of what goes on inside the cavity, as well as, other technologies that help manufacturers, companies and clients check for radiation leakage that the supposed Faraday's cage lets out. The first section refers to thermal vision, visual displays and electromagnetic simulation as the three major categories of methods researchers use to study the energy fields inside the microwave oven. This section also does a broad overview of power meters and how microwave leakage might affect both humans and electrical devices. In the last section of this chapter, the new developments in solid state cooking, and their characteristics, are mentioned and compared with the magnetron using ovens.

Chapter 3 presents the theory of each stage of the proposed probe and it's divided in two sections, Antennas and RF to Direct Current (DC) Conversion. The first section starts with a summary on antenna theory followed by an introduction on metamaterials. To finish this section, an explanation on what defines electrically small antennas and some studied examples that were later on designed and adapted to the work frequency and substrate. The second section is composed by a theoretical overview on RF to DC converters and a more specific analysis on how the proposed configurations operate.

Chapter 4 is where both the simulation and measurements performed are displayed. The antennas were designed with the help of Computer Simulation Technology (CST) software and the RF to DC circuits were designed with the help of Advanced System Design (ADS) software. Throughout the chapter, some commentaries about each presented simulation and/or measurement are also given to clarify several aspects about them.

1.3 Original Contributions

This dissertation provided opportunity to submit two different papers:

G. D. Rosa, N. B. Carvalho, "High Power Diode-Based Rectenna" in Second URSI Atlantic Radio Science Meeting - 2018 (AT-RASC) in Gran Canaria, Spain;

G. D. Rosa, N. B. Carvalho, "High Power LDMOS-Based Rectenna" for 2018 IEEE Wireless Power Transfer Conference (WPTC) in Montreal Quebec · Canada.

Chapter 2

The Inside and Outside of the Microwave Oven

This chapter presents some of the many measuring systems that have been used to represent the electromagnetic field inside the cavity and to measure microwave ovens' emissions/leakage. A small explanation about Specific Absorption Rate (SAR) levels, why they are important and some entities related to this are also presented.

Finally, some insight on the solid state cooking technology, its advantages and differences compared to microwave ovens that use a magnetron. This section is based on Ampleon's RF solid state cooking white paper, [3].

2.1 Measuring Systems

2.1.1 Internal

The systems that demonstrate the power density inside the oven's cavity use different types of technologies to give a visual representation of the electromagnetic field. Technologies like infrared thermal imaging, arrays of LEDs (or neon lights) to display field patterns and computer simulations of the oven system (completely or by parts).

In [4] a thermal image of a tray (Figure 2.1) clearly shows a difference of around 40°C between the outer part of the food and its centre. This leads people to think microwave ovens heat the outside layers of food just like conventional ovens. This is wrong! Radiation penetrates food and makes molecules vibrate which generates heat, but the uniformity of

the heating will depend on the material composition and size. For example, the mashed potato in figure 2.1 has a very uniform composition so its molecules would vibrate equally (be uniformly heated) if they were excited with the same power intensity.

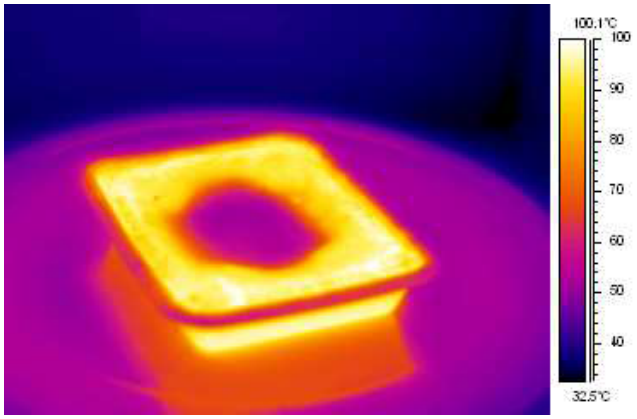

Figure 2.1: Thermal image of a tray of mashed potato, [4].

However, the power source is external to the food and from the moment the radiation penetrates the food the power level will drop, due to losses, which means the inside of the food will be excited with less power than the outside, making it look like the microwave oven heats food from the outside. But if, for example, some kind of food is more liquid on the inside (like many desserts), the centre of this food will be better heated since it has a bigger amount of water molecules. This is exactly the opposite of the previous example, proving the microwave oven doesn't heat neither from the outside in nor from the inside out. Because of the way microwave ovens heat, in [2] it is discussed that food should be cut thinner than the radiation penetration depth for a more uniform cooking.

Also, since the microwave oven's cavity is a resonant cavity, a standing wave pattern (as in figure 2.2) will most likely be formed. This means there will be cold zones near the null spots or nodes (represented with blue colour) and there will be hot zones on the peaks or anti-nodes (red colour), which creates even more differences in the external (to the food) power source and, consequently, in the power that excites each portion of the food.

This standing wave pattern is extremely complex because it's three dimensional, and also because of other aspects that can influence the electromagnetic field, which are discussed in [5], like when something that absorbs or reflects RF energy is put inside the oven, when the cavity resonance is not exactly at the magnetron frequency, when some microwaves are coupled back to the magnetron or absorbed by the walls.

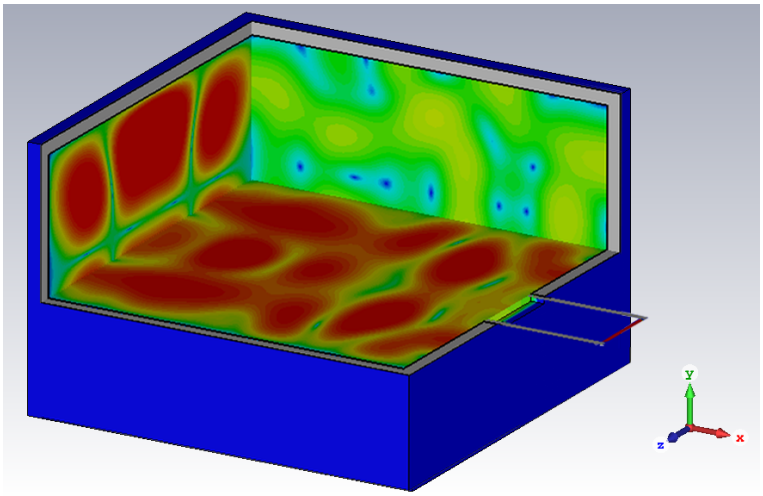

Figure 2.2: Example of a 3 dimensional standing wave pattern made using CST.

In figure 2.3 another thermal image of an experiment mentioned in [5] can be seen where "a glass plate with a thin water film was placed at a height of 8 cm and heated for 15 s with a microwave power of 800 W without using the turntable". This clearly shows different temperature levels throughout the water film confirming there is a standing wave pattern which will radiate some areas more then others.

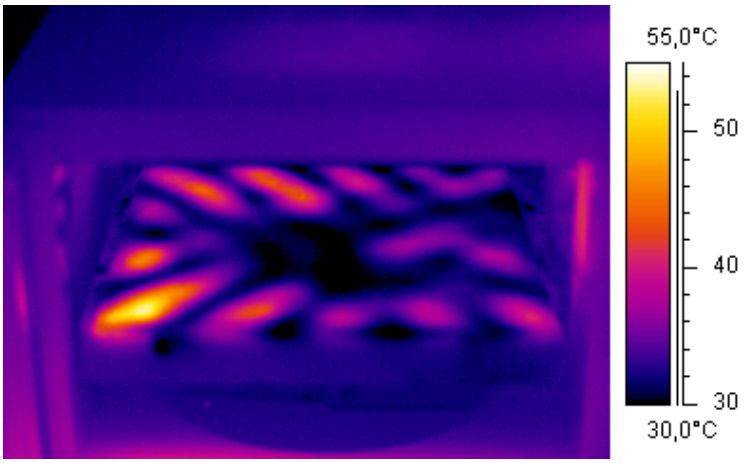

Figure 2.3: Thermal image demonstrating hot and cold spots on a water film, [5].

The two most common structures used to reduce this uneven distribution of RF energy are a turntable placed at the bottom of the cavity, sort of like a plate, and a metal fan on the top of the cavity. The first rotates the food, shifting it through the different hot and cold zones, to try and even the radiation level in every point of the food. The second

redirects the waves emitted by the magnetron, changing the electromagnetic pattern to make it more uniform and so heat the food more evenly. In [2], a uniformity test was conducted to show the difference between not having any structure influencing the field and having the turntable or the metallic stirrer (figure 2.4).

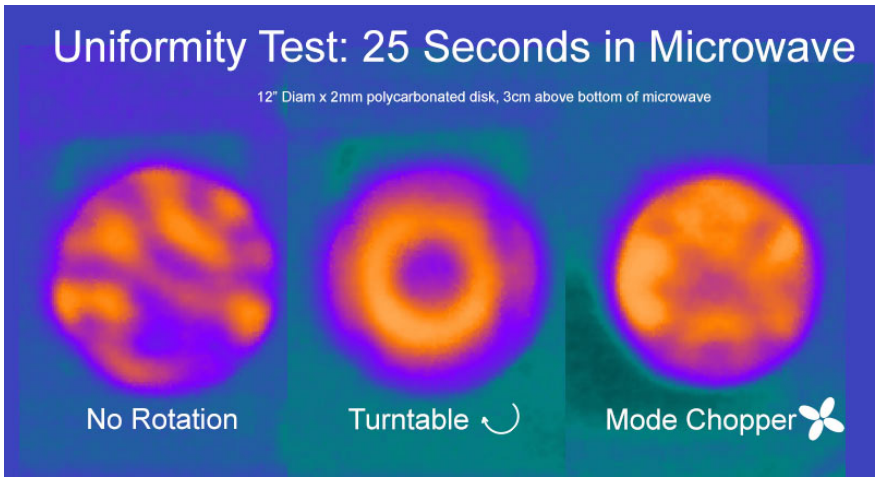

Figure 2.4: Thermal image of a uniformity comparison, [2].

Another way to visualise the electromagnetic field is through the help of visual aids like LED boards and neon lights. In figure 2.5, an example of the first is shown, much like the one in [3] where system architect Robin Wesson, from Ampleon RF Power Innovation, explains that the electromagnetic field inside the cavity can be seen by turning the oven on. This applies power to a "number of neon lamps" or, in this case, a "field pattern detector" board. This board is composed by an array of LEDs that uses three colours, "each connected to a short antenna in the X, Y or Z polarisation planes".

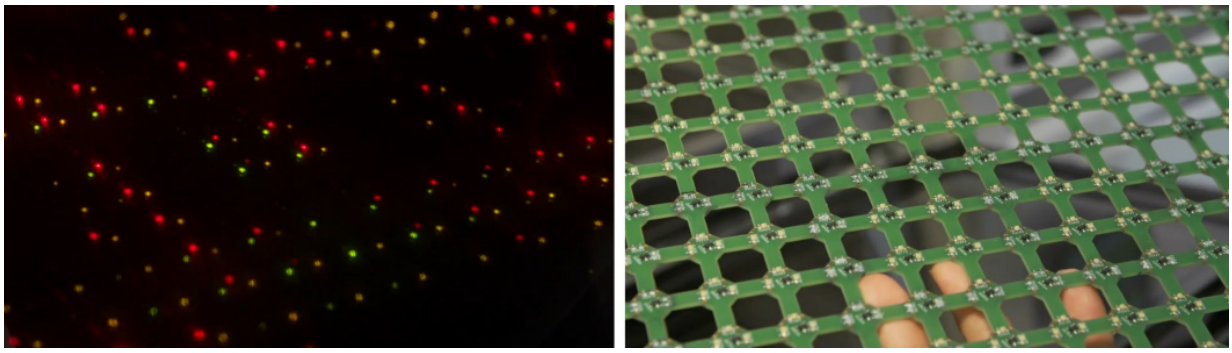

Figure 2.5: Tricolour LED board, [6]. On the left is a shot of it inside the oven.

Since none of the previous examples lets the developers control the electromagnetic field, only lets them observe it, most studies are conducted with the help of simulation softwares. These programs allow developers to optimise by performing slight changes to all the parts that the oven is composed of. Either the cavity's size, the magnetron, the power source, the material, the position of the waveguide, etc. Of course, this complex system takes a while to simulate, but it's still much, much faster then physically changing anything in the microwave oven, redesigning it and reconstructing it to, then, check again and see if it is better or not. Needless to say it is very much less expensive when the only thing being spent is computing power.

CST published an article [7] where it is explained how to simulate the microwave oven system. Starting with the magnetron (left side of figure 2.6), tests of temperature, output power, magnetic field, electric field and frequency spectrum were conducted to design and optimise it. However, the magnetron is not going to be in empty space, the cavity of the microwave oven will influence the electromagnetic field and so will anything that absorbs and reflects microwaves that is put inside the cavity. With this in mind, the image on the right of figure 2.6 shows the electric field inside the oven with a "test load consisting of a cylinder of water" ([7]) which will, as said before, absorb the majority of the RF energy.

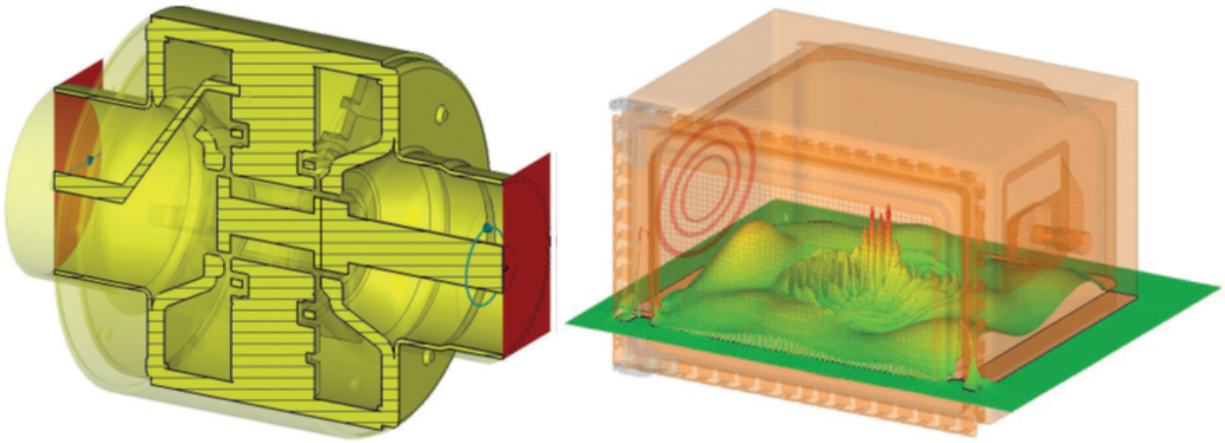

Figure 2.6: "The set-up of the ports and monitors" of a magnetron's design on the left, [7]. "The electric field within and around the oven" on the right, [7].

The physics department of the University of Aveiro published an article, [8], where a study about how the magnetron's frequency, material's dielectric constant and losses change the electromagnetic field pattern inside the cavity. They also look into tempera-

ture and how its variation influences radiation absorption. Even though these experiments are simulated, they clearly show that these microwave oven characteristics affect the electromagnetic field inside the cavity, which add up to the ones mentioned above. As an example, one of the experiments is shown in figure 2.7 where the simulated electric field inside the microwave oven cavity at frequencies 2.45 GHz, 2.2 GHz and 2.7 GHz (top, bottom left and bottom right, respectively) can be seen.

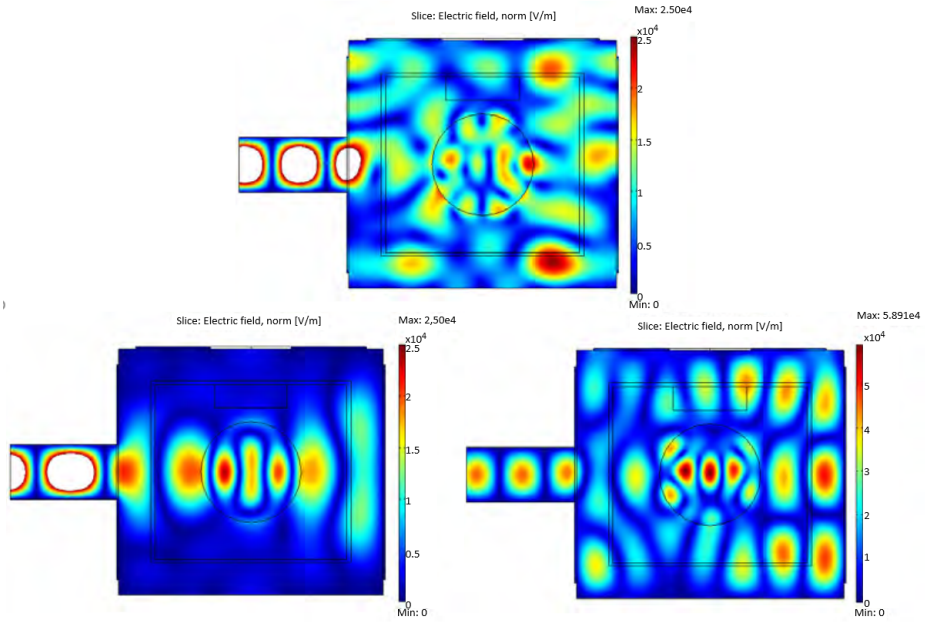

Figure 2.7: Simulation display of the electric field at 2.45 GHz (top), 2.2 GHz (bottom left) and 2.7 GHz (bottom right), [8].

There are still a lot more examples of ways to visualise and analyse the RF energy that flows inside this cooking appliance either academical, industrial or amateur, but most of them revolve around these three main categories.

2.1.2 External

The first microwave ovens' doors were closed by forcing their metal against the cavity's metal structure. Although effective, with time this contact would get worse and, consequently, let out more radiation. This leakage problem was resolved by incorporating a $\lambda/4$ choke to short circuit the RF energy trying to leak out through the door, [9].

In 2004, Kerry Parker and Michael Vollmer wrote about the microwave ovens saying "An estimated 95% of Americans own one and 75% of them use it every day", [1]. In Europe, the microwave oven is not used as much but still a lot of people use it every day. This might not be so advisable because daily exposure could harm your eyes or your central nervous system and cause skin diseases, temporary sterility and cardiovascular problems, [10]. All this is due to electromagnetic leakage which, according to [11], also affects the wi-fi networks, since it radiates "regardless of whether the channel is free or not" and because together with the other interfering devices, mentioned in [11], generates a wideband interference affecting multiple wi-fi channels. To study and check the veracity of these statements, various devices/tests to measure the electromagnetic leaking radiation were made and some of them are addressed here.

In regard to the inference on wi-fi a set of experiments with two different microwave ovens, a router (Cisco WAP4410N IEEE 802.11/n/b/g) and two different laptops has been conducted, [12]. The microwave oven was placed between the laptop and the router in several places which vary in height (from the ground, 0 meters, to the router's height, 0.6 meters, and 1 meter above the ground) and distance from the router (1 meter, 5 meters, 9 meters and the laptop was 10 meters away) as it is represented in figure 2.8. This study concludes that the interference of the microwave oven leakage on the wi-fi signal strength is insignificant, although, it increases the number of errors in the data transmission.

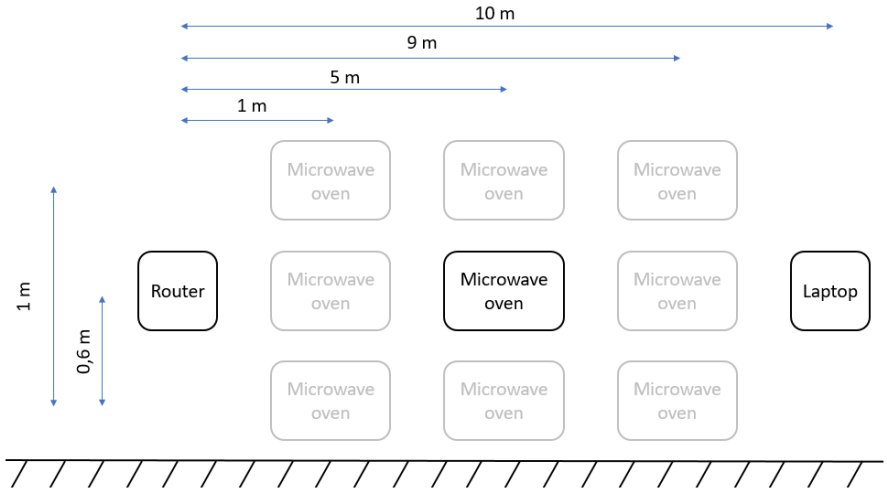

Figure 2.8: Representative block diagram of the experiment done by Noor Qadar, [12], and his team on the interference of microwave oven's leakage in wi-fi networks.

On the other hand, to check the Faraday's cage, which the cavity of the microwave oven is supposed to be, several tests and measurements can be made. When a microwave oven is ON, being anywhere closer then 30 centimetres is not advised! Either way, a well functioning oven should not emit more than 5 mW/cm^2. With this in mind, manufacturers need to check for electromagnetic radiation that might leak out of the cavity. An old microwave oven should also be checked, since its door and overall structure degrades with time and use. To do this, some kind of power meter should be used 5 centimetres away from the chassis and in several points around, as it is shown in figure 2.9, like the experiment in [10]. This experiment was done inside a chamber room with only one of the six measured microwave ovens at a time and one electric field probe so there wouldn't be any kind of interference from other devices in the measurements. Only two of these ovens had leakage levels above 1 mW/cm^2 and only one exceeded the 5 mW/cm^2.

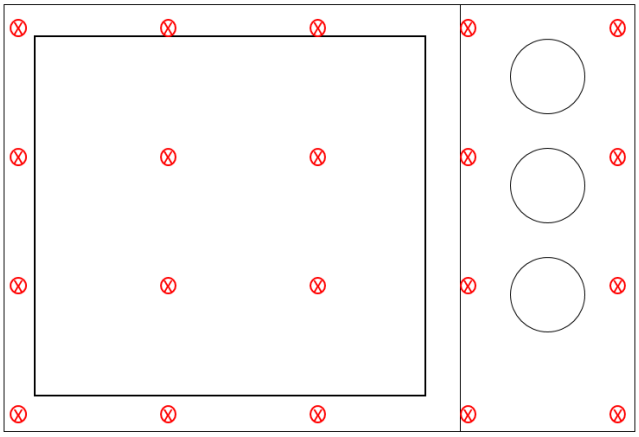

Figure 2.9: Points where a power meter should be placed to measure the leakage radiation from a microwave oven, based from [10].

This 5 mW/cm^2 level is a safety standard which is based on an emission limit that is related to the American National Standards Institute (ANSI) exposure limit, [13], and the 5 centimetres from the door are due to a distance "that is as close as the human eyeball can come to the oven", [14]. This limit started out at 10 mW/cm^2 but, with health institutes persuading to lower this value, a limit of 1 mW/cm^2 at manufacture and 5 mW/cm^2 at sale, both at 5 centimetres, was since then standardised. This is referred in emission standards like the ones issued by the International Electrotechnical Commission (IEC), [9], and the Australian Standards Association, [15].

The International Commission on Non-Ionizing Radiation Protection (ICNIRP), [16], mentions that the exposure to electromagnetic fields, that produce an absorption rate greater than 4 W/kg, could diminish the body's thermoregulatory capacity and produce dangerous levels of tissue heating. Health and other biological effects caused by radiations in the frequency span of 10 MHz to 10 GHz are consistent with responses to a rise in body temperature of 1 °C. This temperature increase is caused by a whole-body exposure to a SAR of approximately 4 W/kg for 30 minutes (SAR is the amount of RF energy absorbed per mass unit by a body close to an emitting device). Because of this, the chosen whole-body average SAR for adequate protection to professional exposure is of 0.4 W/kg and, with an additional factor of 5, to public exposure is 0.08 W/kg, as shown in table 2.1.

In agreement with ICNIRP, another entity related to this matter, Australian Radiation Protection and Nuclear Safety Agency (ARPANSA), set its general public limit at 2.45 GHz for a whole-body exposure to 0.08 W/kg. This is determined by the SAR that induces an increase in body temperature of 0.02 °C which is caused by the whole-body exposure limit of 10 W/m^2 (1 mW/cm^2), [17].

Exposure characteristics	Frequency range	Whole-body average SAR (W/kg)	Localized SAR (head and trunk) (W/kg)	Localized SAR (limbs) (W/kg)
Occupational exposure	10 MHz - 10 GHz	0.4	10	20
General public exposure	10 MHz - 10 GHz	0.08	2	4

Table 2.1: Adapted from table "Basic restrictions for time varying electric and magnetic fields for frequencies up to 10 GHz.", [16].

A very common misunderstanding has been passed on due to the fact that the emission limit is determined by the exposure limit. People think the emission limit is a safety border, which compromises the user's safety if exceeded, but, as [9] says, "The emission limit is primarily a manufacturing specification, exceeding the emission limit does not imply that safety will be compromised. Compliance with safety limits is determined by referring to relevant radiofrequency exposure standards and not emission limits".

To demystify this, companies work on the design of power meters, so users and other companies can check microwave ovens in different environments. One of those is Microwave

Safe Australia which inspects microwave ovens in workplaces and provided measurements, from the approximately 12000 ovens they inspect per year, to [9]. These state that only 0.8% of the ovens have radiation leakage levels greater than the exposure limit mentioned above.

ARPANSA also did some measurements together with EMC Technologies, [9], to test how the leaked radiation behaves with distance and how it affects the human body. To do this, a gel equivalent to a muscle tissue is put inside a phantom to model the human body. They also forced the door of the microwave oven to impose a 5 mW/cm^2 emission level before testing with a "computer controlled robot-mounted probe" to monitor the field strength in a phantom, placed next to a leaking microwave oven. This test proves, if a certain distance is kept, there is no harm even with a leaky microwave oven. Since at 5 centimetres the SAR was 0.256 W/kg and at less then 1 millimetre it was 7.95 W/kg which, as estimated, would give a 0.0056 W/kg SAR 30 centimetres away, figure 2.10. This article goes on to estimate what level of leakage would be needed to surpass both the head and torso, and the limb SAR limit.

Figure 2.10: Microwave oven leakage SAR levels, adapted from [9].

In another article, a test to see if some of the most common (and cheap) electromagnetic field detectors are a reliable measuring system or if they either say there's no leakage, when there actually is, or give levels much greater then the real ones, [18]. The International Microwave Power Institute (IMPI) shares their results through this article, where a mi-

crowave oven was not used since its leakage varies significantly from oven to oven due to its design and structure. Instead "a software-controlled instrument was built to recreate the function of an "artificial leak" with settable values and polarisations" which was then put inside an anechoic chamber together with the detector under test. The ETS-Lindgren's HI-1710A Microwave Oven Survey Meter was used as a reference field detector to compare with the other 7 measuring instruments. Only one of these 7 meters had a reliable response and in range power detection. All the other power measures were too high which would lead people to think they have a malfunctioning oven, that is not safe when it's perfectly fine, or power measures too low that make people feel safe and continue using the oven even though it's leaking radiation above the SAR limit.

Finally to show as an example of what power detectors look like figure 2.11 shows the reference field detector used in the previous article (bottom left), the power meter that, also in the previous article, had reliable results (top left) and an example of a professional power meter by Narda Safety Test Solutions that can use different probes for different frequencies, NBM-520 taken from its datasheet, [19].

Figure 2.11: Example of power probes. On the top left is the measuring instrument that IMPI proved to be reliable, [18], and on the bottom left is the ETS-Lindgren's HI-1710A Microwave Oven Survey Meter. On the right is Narda's broadband field meter: NBM-520, [19]

2.2 Solid State Cooking

Solid state cooking is a new type of cooking that takes advantage of the breakthroughs in the RF engineering and communication fields. Control of energy delivery is its main characteristic.

High power transistors are now capable of delivering power levels comparable to those of the magnetron. They have been increasing efficiency and power density in the last generations of developments in the RF and communication's engineering.

Even though the magnetron's design has been optimised through the years to have a high power delivery with good efficiency at a decent cost, its accuracy and control fall short of the average level of today's radar technology. Furthermore, the magnetron has a variability in performance that cannot be accepted in today's standards.

Solid state system have high flexibility, in the sense that, they have high power control performance that can adapt to each food. This matching is done through feedback mechanisms that match the power delivered in frequency and phase for improved heating capable of adjusting to each food. Another aspect that both the magnetron and solid state amplifiers share in common is variation in power delivery with temperature. However, the new technology utilises the feedback mechanisms to properly correct the power and gain variations with temperature. This is another feature that comes from communication systems, as well as, being able to perform equally in the first, second, tenth and one hundredth operation. This cannot be done with a magnetron that, aside from its variability, has a limited lifetime and its output wattage deteriorates with time and use.

Different foods represent different loads which, in turn, represent different frequency and phase for optimal heating. By sensing the reflected power, either from the cavity or from the load, each food, and any changes with time, can be 'sensed'. This represents a new approach to sensing, where the electromagnetic power source can adjust itself to appropriate cooking time, power, phase and frequency to perform a specific task. This increases the amount of possible cooking sequences in order to perfectly heat different types of food.

Due to the resonant properties of the cavity, it doesn't matter if the power source is a magnetron or a solid state amplifier, there will still be standing wave patterns. This pattern will variate with load and, although visual aids can help visualise it, they are not very convenient since they can't demonstrate how the pattern changes with different loads.

The RF Energy Alliance is a technical association that clusters several companies in order to achieve a RF energy power source that is clean, highly efficient and with controllable temperature and contributing to a quality of life in many areas, just like the solid state cooking. Some of these solid state cooking devices have already been introduced, like WAYV's portable solid state cooking device, NXP's Sage solid state cooker, GOJI's RF oven, among others.

Figure 2.12: Examples of the new solid state cooking appliances (from magazines, symposiums and other articles throughout the web).

Chapter 3

Field Detector Probe

This chapter presents the research done in order to design the proposed measuring system. First some theory about antennas, followed by a study about metamaterials, their characteristics and why they could be a good choice for this application, and electrically small antennas and why there has been an increasing interest in this type of antennas.

Secondly, some theory involving RF to DC conversion is presented together with specific characteristics that the components used need to have for the application proposed, accompanied by a comparison between typical and proposed converters.

3.1 Antennas

As said by Constantine Balanis, [20], "the antenna is the transitional structure between free-space and a guiding device", "The guiding device or transmission line may take the form of a coaxial line or a hollow pipe (waveguide), and it is used to transport electromagnetic energy from the transmitting source to the antenna, or from the antenna to the receiver."

3.1.1 Antenna Theory

Nowadays, there are many books about antennas that explain and help many students, researchers, companies and others to design their own antenna. This section is based on one in specific, the *Antenna Theory: Analisys and Design* by Constantine A. Balanis [20], with citations from the *IEEE Standard for Definitions of Terms for Antennas*, [21].

Antennas are used as an interface between a communication system and free-space. In order to do this, there needs to be a variation of current in time or an acceleration (positive or negative) of charge. This can happen thanks to a source which produces electric lines of force, that set in motion free electrons inside a wire. When this happens, the charges are accelerated on the extremity connected to the source and decelerated on points in the wire, where a accumulation of charges is produced (impedance discontinuities), which then radiates an electromagnetic field on both extremities and along the wire.

When a transmission line consists of two conductor lines, and a source applies voltage between them, an electric field is created. Along each point of the transmission line, the electric lines of force of this field are tangent to it, their strength depends on the field intensity and, like in the single wire, they set the free electrons in motion, which then generates a current and, consequently, a magnetic field intensity. This electromagnetic field is guided through the transmission line, until an enlargement of the two conductors occurs. If the distance between the conductors becomes large enough, the field will radiate to free-space, like the representative example in figure 3.1.

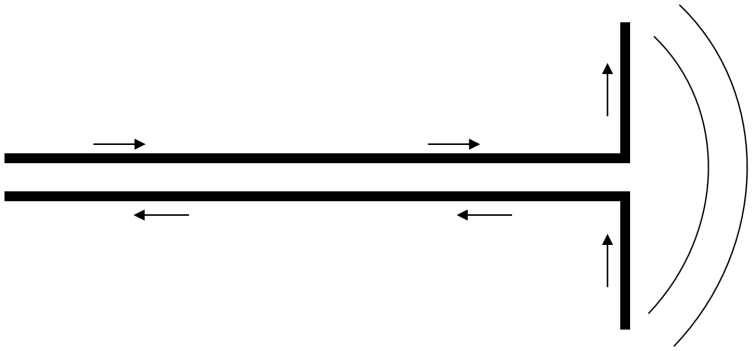

Figure 3.1: Representative example of a transmission line ended in a frequently used dipole. This sketch is based on a similar one from [20].

Antennas have several fundamental parameters, such as, radiation pattern, power density, radiation intensity, beamwidth, directivity, gain, efficiency, bandwidth and polarisation, which are discussed here.

The antenna's **radiation pattern** can be described as "a mathematical function or a graphical representation of the radiation properties of the antenna as a function of space coordinates". One of these properties is the spatial distribution (2D or 3D) of the transmitted energy on a circle or sphere of constant radius.

The amplitude field pattern is the electric field strength on a constant radius surface and the amplitude power pattern is a graphical representation of the variation of power density on space in a constant radius surface. The first pattern is represented in linear scale and is used to plot the electric (or magnetic) field's magnitude. The second pattern can be represented both in linear scale and in dB. In linear scale, the power density represents square of the electric (or magnetic) field's magnitude and in dB represents, in decibels, the electric (or magnetic) field's magnitude. All the three representation plots are in function of the angular space.

Generally, "the radiation pattern is determined in the far-field region" which is one of the three regions that define the space surrounding an antenna, together with the reactive near-field and the radiating near-field. These regions have clear differences, but, when transitioning from one to another, there are no sudden changes in the field configuration. These transitions are defined by the largest dimension of the antenna, D, and the wavelength, where the reactive near-field is the sphere with a radius that verifies the condition $R < 0.62\sqrt{D^3/\lambda}$, the radiating near-field is the region in between the reactive near-field and the far-field, which verifies the condition $0.62\sqrt{D^3/\lambda} \leqslant R < 2D^2/\lambda$, and, finally, the far-field region is defined by the condition $R \geqslant 2D^2/\lambda$.

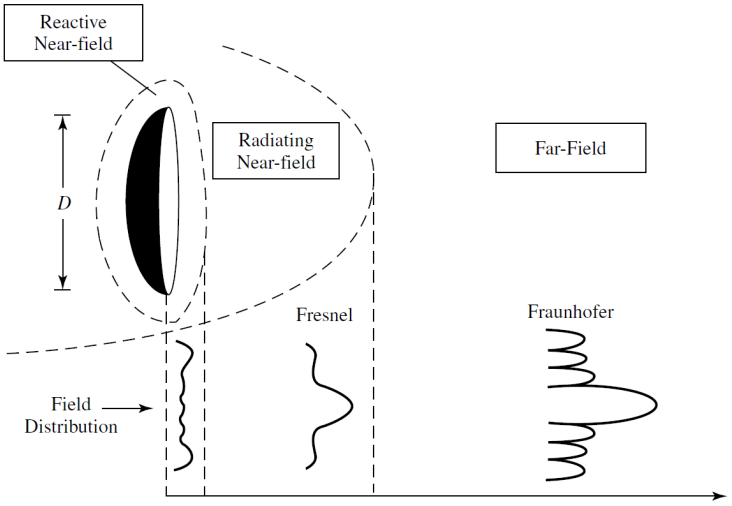

Figure 3.2: Evolution of the antenna's amplitude pattern shape in the different field regions (adaptation source, [20], original source, [22]).

A clear difference between the three regions is the amplitude pattern shape, as seen in figure 3.2. These changes in shape, due to field (magnitude and phase) variations, are

progressive, but, for the purpose of clarity, each region has a corresponding shape. In the reactive near-field, this shape is almost uniform, with only some minor variations. After that, in the radiating near-field region, the shape smooths up and starts to form lobes. Finally, as the observation moves to the far-field region, the amplitude pattern shape has well formed lobes.

These lobes are very important in determining some antenna parameters, like radiation intensity, beamwidth and directivity, and can be defined by their intensity and location. The major lobe is the one where the radiation is maximum, although, some specific types of antennas can have more then one. It's also used as a reference for directivity and to designate other lobes, such as, minor, side and back lobes. The latter's direction is approximately 180^{o} from the main (major) lobe. Minor lobes are all those that aren't the major lobe (usually represent undesired radiation) and the side lobes are those adjacent to the main lobe and tend to be the biggest minor lobes. The power density of the minor lobes is, commonly, expressed in relation to that of the major lobe.

Another difference between regions is noticed in the **power density**, which is complex and expressed in W/m^2. Its imaginary part is dominant in the reactive near-field, while the real component is dominant in the far-field, [23]. The power density in function of direction is the mentioned antenna's power pattern.

The power pattern presents another parameter, the **radiation intensity**, which is "the power radiated from an antenna per unit solid angle". This means, its level depends on direction and is maximum on the major lobe and minimum on the nulls that limit each lobe.

The major lobe, where the radiation intensity is maximum, is where another parameter of the antenna pattern can be defined. The **beamwidth** is determined by the angle between two directions of equal radiation intensity. The two most common definitions are the Half-Power Beamwidth (HPBW) and the First-Null Beamwidth (FNBW), where the first is determined at one half of the beam's maximum power and the second at the first nulls of the pattern (Figure 3.3(a)). Other beamwidths can be referred on several values bellow the maximum, but when it's not specified the beamwidth refers to the HPBW.

An isotropic radiator is used as a base reference in order to compare antennas. This type of radiator, which is defined as "a hypothetical, lossless antenna having equal radiation intensity in all directions", doesn't exist, but is very useful to express directivity and gain of real antennas.

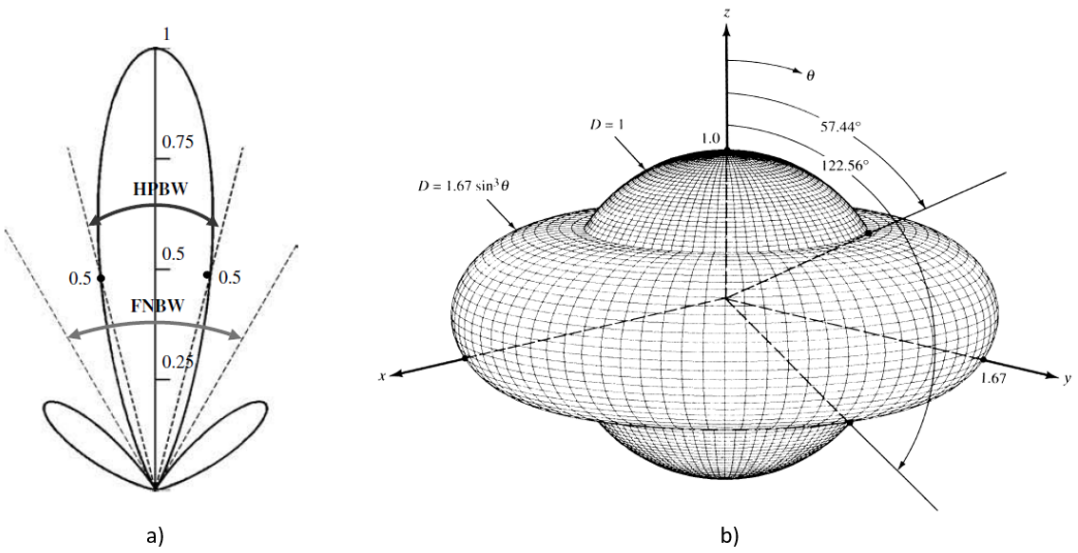

Figure 3.3: a) Two-dimensional pattern adapted from [20]. b) Three-dimensional pattern of an isotropic radiator and a $\lambda/2$ dipole, [23].

The **directivity** is a figure-of-merit that compares the radiation intensity, in any direction, of the isotropic radiator to that from a given direction of an antenna. The directivity of an antenna can be determined in all directions, but, when not specified, it's relative to the maximum radiation intensity direction, which gives the maximum directivity. An example of this comparison can be seen in figure 3.3(b), where the 3D isotropic pattern is compared to a $\lambda/2$ dipole's pattern.

The **gain** parameter of an antenna is similar to the directivity but differs in the power ratio in the sense that it considers the antenna's efficiency. Directivity compares the antenna's radiation intensity in a specific direction to the radiated power from the isotropic antenna, whereas gain compares to the accepted power that is radiated by the isotropic antenna. If the antenna were to be ideal, i.e. lossless, the gain would be equal to the directivity. The default direction is that of maximum radiation, where the gain is maximum.

In terms of antenna **efficiency**, the approach that relates gain with directivity is the conduction and dielectric efficiency (antenna radiation efficiency) that takes into account the conduction and dielectric losses of the antenna, i.e. relates the antennas input power with the radiated power. The total antenna efficiency also considers the mismatch losses of the antenna, that, when perfectly matched, has a total efficiency equal to the radiation efficiency.

Bandwidth is a range between certain frequencies that depends on different characteristics and so cannot be described in a unique way. The two main categories are denominated as pattern bandwidth and impedance bandwidth. The first is determined by gain, side lobe level, beamwidth, direction or polarisation, while the impedance bandwidth is determined in relation with input impedance or antenna radiation efficiency.

Polarisation is an important factor that is, sometimes, overlooked, specially in power budgets. This antenna parameter varies with the distance from the centre of an antenna and can be described as "that property of an electromagnetic wave describing the time-varying direction and relative magnitude of the electric field vector". The extremity of this vector, in function of time, will form a curve that, if seen through the direction of propagation, will form three types of polarisation: the elliptical polarisation and two special cases of that, the linear and the circular polarisations. Linear polarisation is achieved when the electric field vector, on a certain point in space, has an orientation aligned with a straight line at every moment in time, i.e. the field vector either has only one component or the x and y components have 0^o, or any multiples of 180^o, phase difference. Similar to the latter is the circular polarisation, that instead of being aligned with a straight line, is aligned with a circle. To achieve this, the field vector components have to be orthogonal (have odd multiples of 90^o of phase difference) and of the same magnitude. Last, but not least, the elliptical polarisation comprises the other combinations of the field vector components. To achieve this polarisation the x and y components must either have the same magnitude and a phase difference that is not any multiple of 90^o or have different magnitudes and a phase difference that is not any multiple of 180^o. If the polarisation of an incident wave is not aligned with the polarisation of the antenna, there will be polarisation losses and the power absorbed by the antenna will not be maximum.

Upon the design of an antenna, one does not take into account all these parameters simultaneously, since that would be extremely complex. Generally, an antenna is optimised for large or narrow bandwidth, maximum efficiency, maximum gain or another specific characteristic to a specific application. In this dissertation, the goal is to have a small sized antenna with an omnidirectional pattern. The latter is a pattern that distinguishes itself for having a non directional pattern in a certain plane and a clearly directional pattern in all orthogonal planes. These are, generally, single 360^o lobe patterns, where the major lobe renders a plane circle.

3.1.2 Metamaterials

Metamaterials are "composite materials that mimic known material responses or that qualitatively have new, physically realizable response functions that do not occur, or may not be readily available, in nature", [24].

First mentioned around the turn of the century (1900s), these "man-made twisted structures", [24], have been studied in various ways throughout the century for several different applications. Around the 80s, microwave radar technologies were turning their eyes on these artificial materials. Relevant types of this kind of material are Double Negative (DNG), Negative Index of Refraction (NIR) and Electromagnetic Band Gap (EBG) structured materials, and also complex surfaces like ground planes with high impedance. DNG materials work with elements and gaps between them much smaller than the wavelength of their resonance and their main properties are the effective negative permittivity and permeability. In contrast, EBG materials include distances greater or equal to half a wavelength.

In the microwave region of the spectrum, metamaterials are generally arranged by conductive elements with convenient capacitive and inductive characteristics. This dissertation will review some examples of this, together with size limitations imposed by the definition of electrically small antennas.

3.1.3 Electrically small antennas

With the developments in technology of the last decades and, now more than ever, with 5G and Internet of Things (IoT), antennas for these wireless devices are needed. These antennas need to be small and have wideband characteristics, [25], but these two condition, according to Chu's limit, [26], don't go with each other. A smaller size induces a smaller bandwidth and a wider bandwidth requires a bigger size. Since 1948, this has not been disproved, but researchers have conducted many experiments of these so called Small Form Factor (SFF) antennas, [27].

The SFF term is also used for some devices, like smart phones (which include Bluetooth, Global Positioning System (GPS), wi-fi connection, etc) and sensors for technologies like 5G and IoT, that require electrically small antennas. The latter are antennas smaller then their wavelength at their work frequency, as defined by Wheeler, [28], by having the longest dimension smaller than $\lambda/2\pi$ (radianlength), which means the antenna dimensions satisfy

the following condition

$$ka < 0.5 \qquad , \qquad k = \frac{2\pi}{\lambda} \tag{3.1}$$

Where a is the radius of the smallest sphere involving the whole antenna. Volakis [29] also refers another definition of electrically small antenna that is defined as an antenna that fits inside a circle with one radianlength radius

$$ka < 1 \tag{3.2}$$

Equation (3.2) is based on "the boundary between the near- and far-field radiation for a Hertzian dipole" (whose field solutions are used as a mathematical basis for radiation calculations). In this dissertation, this last condition will be the one used as a determining factor to see if the designed antennas are electrically small or not. At the operating frequency, 2.45 GHz, according to (3.2), $a < 19.5$ mm.

The electrical size influences, not only the bandwidth, but also the efficiency and gain. Other parameters such as permittivity, aspect ratio and the nature of the structure within the antenna affect the performance of an antenna, [27]. The lower the permittivity the higher the performance. If the aspect ratio is close to unity, the performance will be the highest possible. Finally, if the structure within the antenna creates fields, within the smallest sphere involving the whole antenna, that are as uniform as possible, the best performance will be obtained.

3.1.4 Designed Antennas

In the scope of this dissertation, several configurations of antennas were studied. A concise and summarised description of this study is presented here, where the designed antennas and their characteristics are given a greater emphasis. Planar Inverted F Antenna (PIFA)s are used for several communication applications and are designed to have small size since communications devices, like cellphones, require small sized components. PIFA's feed line connects to an orthogonal quarter wavelength line open-circuited on one side and connected to ground on the other side, which form a sort of F shaped line configuration. Many researchers have reported the use of these antennas in various communication applications, [30], [31], [32]. Although, they are normally small, PIFAs have the $\lambda/4$ line, which narrows the impedance bandwidth as well. However, some methods can be used

to reduce its size and widen its bandwidth like introducing slots and adopting meander lines, [33]. Several different configurations of PIFAs were tried (some based on the articles mentioned here) and the one presented in figure 3.4 was the configuration that had the best performance. The coaxial feed is connected through the backside of the antenna and the position of the via, that implements the short circuit to the ground plane was optimised. The widths and lengths of both the feeding and shorting lines were also optimised in order to achieve the best performance (lower S11 at 2.45 GHz, small size and bandwidth of at least 100 MHz around the fundamental frequency).

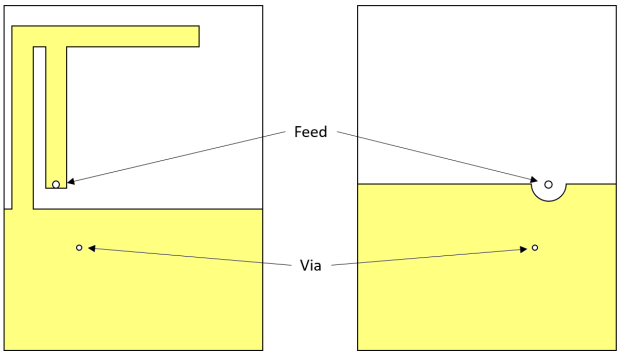

Figure 3.4: Drawing of the designed PIFA.

Another widely used configuration is the planar inverted L antenna. Based on this type of antenna, together with the, already mentioned, technique of size reduction of bending a straight line to create a meander line structure, the antenna that is represented in figure 3.5 was designed with the objective of producing a small sized omnidirectional antenna.

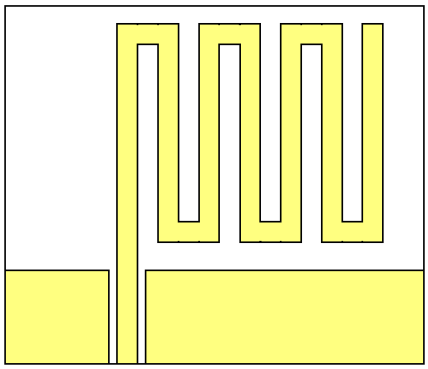

Figure 3.5: Drawing of the designed meander line antenna.

This meander line antenna has the ground plane and the meander line monopole on the same side of the substrate and the backside of the antenna has no copper at all. This configuration could be used in antennas, with special constraints, that would require a single sided structure.

Microstrip patch antenna are made of a metallic patch that, unlike most planar antennas, is on a fully grounded substrate. They are very low profile, adaptable to planar and non-planar surfaces, easy to fabricate and very versatile, [20].

These antennas are also an attractive option for designing electrically small antennas. The one proposed in this dissertation is based on the one produced in [34], where a shorting post together with a Defected Ground Structure (DGS) are proposed to miniaturise the patch antenna so that a lower frequency resonance can be achieved. The miniature patch antenna proposed in this dissertation was optimised for the 2.45 GHz band rather than for having a dual-band behaviour, which lead to reducing the U shaped slot (part of the DGS) that gave a dual-band property to the miniaturised patch antenna proposed in [34]. The positions of the feed and the shorting post (represented by a via in figure 3.6) were also optimised for a better performance at the 2.45 GHz resonance.

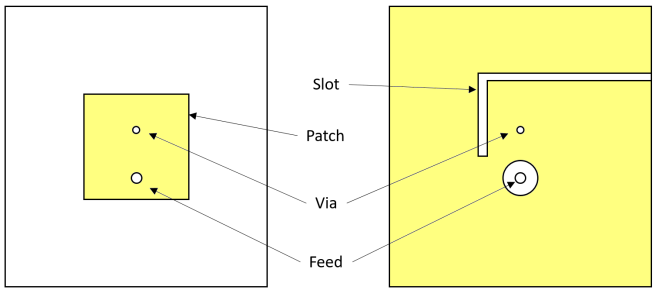

Figure 3.6: Drawing of the designed miniaturised patch antenna.

Antennas for mobile applications should be low profile and have dual-band (or multi-band) properties. An attractive option for that purpose is the loaded monopole. In [35], the use of metamaterial-inspired techniques is report in order to achieve the dual-band characteristic, where the antenna proposed is a Coplanar Waveguide (CPW) fed two-arm monopole with a loaded inductor on top, or simply a T-shaped slot on a rectangular patch, with an interdigital capacitor on the right side. The loaded monopole proposed in this dissertation (Figure 3.7) is an adaptation of the previous one that gives a greater focus on the lower wi-fi band improving bandwidth and reflection coefficient at that band.

Also, this antenna is single-layered with no vias which makes it easy and cheap to fabricate and also applicable to antennas with special constraints that would require a single sided structure.

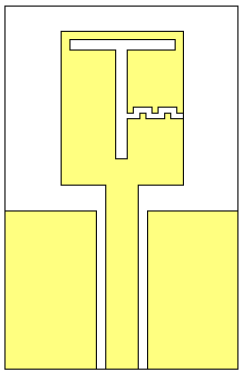

Figure 3.7: Drawing of the designed loaded monopole antenna.

Complementary Split Ring Resonator (CSRR) is also a good technique to improve bandwidth and its geometrical characteristics fit inside compact antenna which makes it desirable for SFF devices. In [36], a radiating strip with a metamaterial-based matching network is proposed. This matching network consists of a CSRR embedded in the ground plane (bottom layer) accompanied by a capacitive flare on the top layer that form a shunt LC network, which, together with the radiating strip, form a double-tuned matching network with improved bandwidth.

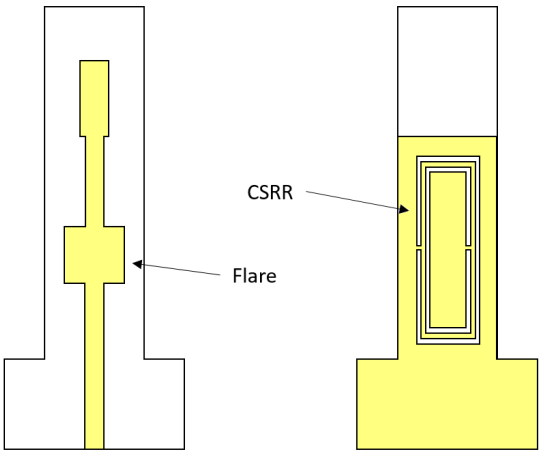

Figure 3.8: Drawing of the designed CSRR loaded antenna.

Some dimensions of the components proposed by the article were too small. With that in mind, an antenna, based on the one that is described, is proposed in this dissertation with wider lines for easier manufacture and shorter overall length to maintain the compact size, figure 3.8.

In antenna design, the techniques mentioned here, as well as others mentioned by the antenna designing community, can be very useful to achieve miniaturisation without disregarding performance, as long as they are made to fit the compact area of the antenna.

3.2 RF to DC Converter

3.2.1 Theory and Configurations

Heinrich Hertz and Nikola Tesla's works gave way to the immense field of research that is Wireless Power Transmission (WPT), [37].

WPT systems consist of two main stages, separated in space, between which the energy flows, the transmission and the reception. The transmission stage is, in general, a base station, but in this dissertation's case, it's just a magnetron that generates and transmits RF energy through a waveguide. The reception stage is a rectenna, which is the combination of an antenna, mentioned above, and a rectifying circuit that converts the transferred RF signal to DC power. This rectifying circuit is preceded by a matching network that acts as a band-pass filter to prevent the harmonics, generated by the non-linear behaviour of the rectifying element, from being radiated through the antenna. On the other side of the rectifying element is a low-pass filter to remove the high frequency components and deliver a DC output voltage. These three components make up the energy-harvesting circuit that, together with an antenna, is represented in figure 3.9, [38].

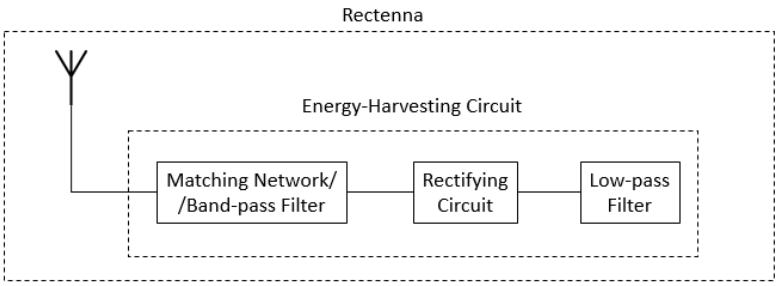

Figure 3.9: Rectenna block diagram adapted from [38].

The most common rectifying circuits involve a number of diodes and capacitors. These diodes are responsible for the non-linear behaviour of RF to DC converters, in the sense that, because of the non-linearity, the impedance will depend on input power, causing circuit matching to be a very difficult task.

Diodes can be characterised by their relation between current and forward voltage, seen in figure 3.10. This relation is subdivided in three sections that are delimited by breakdown voltage, V_{br}, and voltage threshold, V_T. Above the latter, current and voltage are proportional, between V_{br} and V_T the diode is cut-off (there's only leakage current) and for voltage levels below the breakdown voltage the diode will be reverse biased which means it will conduct in the opposite direction, [38].

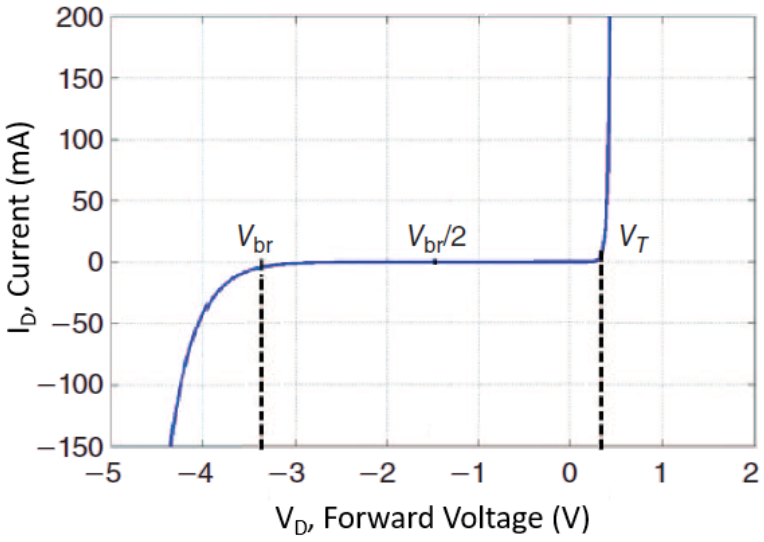

Figure 3.10: Example diode I-V curve adapted from [38].

Efficiency and sensitivity are the two main parameters of energy-harvesting circuits. The latter is determined by the minimum output DC power necessary to feed a specific circuit, be it a sensor, a microcontroller, etc. The output DC power is determined by the square of the output DC voltage divided by the load resistance and, in turn, also determines the power conversion efficiency. Energy-harvesting circuit's efficiency is usually referred to the available power delivered by the antenna, $\eta = \frac{V_{outDC}^2}{P_{av}.R_L}$. This definition doesn't take into account the rectifiers reflections focusing on the end-to-end delivered power. For large signals, the main loss sources are reverse breakdown voltage, impedance mismatches, harmonics (greater the input, greater the harmonic losses), among others.

Efficiency is also influenced by the rectifier circuit's topology, like the Dickson, the Cockcroft-Walton charge pumps or more simple ones like a single diode half-wave rectifier or a single shunt rectenna, [38]. SPS and other WPT applications deal with high levels of input power, unlike Ultra High Frequency (UHF) applications, such as RFID tags and other low power operating systems. For this reason, they don't require multistage topologies, therefore, single diode rectifiers (single stage) are a very common approach when it comes to designing the rectifying circuit. The RF to DC converter proposed in this dissertation is based on a single stage Dickson charge pump, as will be demonstrated later.

An alternative to diode-based rectifiers has been reported in the scientific community, [39], [40]. These make use of a Pseudomorphic High Electron Mobility Transistor (pHEMT) and its non-linear behaviour by driving the transistor's drain, which then generates DC, fundamental and harmonic frequency components. Finally, with the use of a low-pass filter, just like diode-based rectifiers, the high frequency components are filtered and a DC output voltage is delivered. This dissertation proposes a rectifier circuit based on the one represented in figure 3.11 from [40].

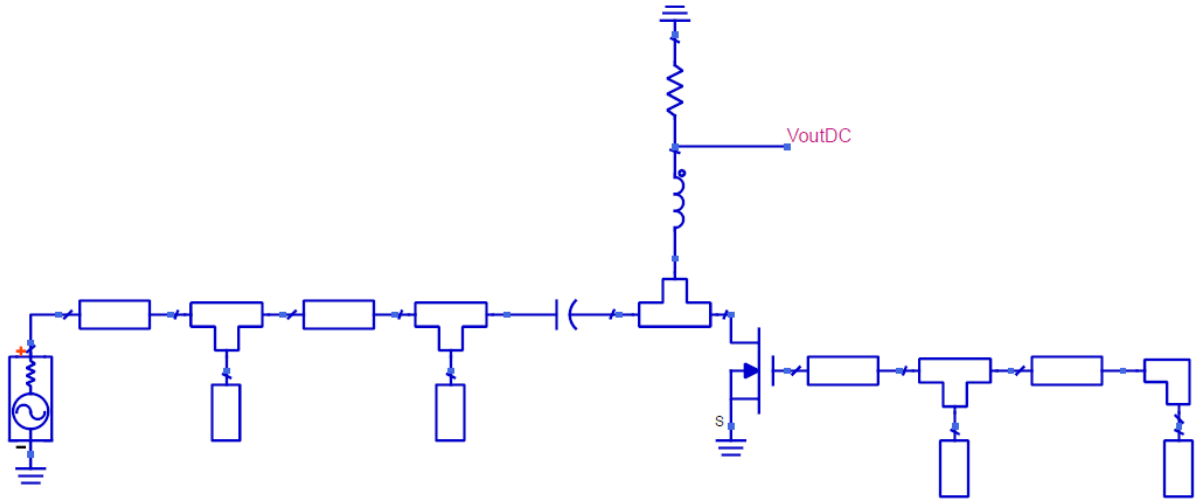

Figure 3.11: pHEMT-based rectifier topology adapted from [40].

3.2.2 RF High Power Diodes and Transistors

A power measurement probe for electromagnetic fields usually works with low power applications, like routers, cellphones and other communication devices, but in this case its

power levels go from 80 W to 800 W, making typically used components unusable.

With that in mind, the selected diodes were SMP1302-79LF and SMP1304-79LF from Skyworks. The LDMOS transistor BLC2425M8LS300P from Ampleon is used in the new RF cooking appliances and was the one used for the transistor-based rectifier. Figure 3.12 shows the RF components chosen taken from their datasheet and, in the transistor's case, from Ampleon's website.

Figure 3.12: Diodes and transistor used for proposed rectifiers.

Chapter 4

Simulation and Measurement

This chapter focuses on the simulated designs and the conducted measurements. Firstly the antennas that were studied (described in the previous chapter) and the monopole antenna used. Secondly, the RF to DC converters that were design for the first and second "tests".

4.1 Antennas

As mentioned in chapter 3, the antenna configurations chosen to study and design were 5, a PIFA, meander line, a patch, loaded monopole and CSRR loaded antennas. These 5 designs were simulated using CST software to validate the research mentioned in section 3.1.3. A monopole was designed, printed and measured to serve as the antenna for the power probe.

4.1.1 Simulated

The following antenna designs are based on the articles and studies mentioned in section 3.1.3. These antennas were designed with a FR-4 substrate, with a 1.6 mm thickness, a 4.3 dielectric constant, a cladding of 35 μm and a 0.025 loss tangent (values taken from CST's FR-4 (lossy) substrate characteristics).

With the help of the Parameter Sweep and Optimizer tools provided by CST Studio Suite, the following antennas were modelled based on similar (previously mentioned) antennas and then adapted to the substrate and desired frequency.

The PIFA's 3D view is represented in figure 4.1.

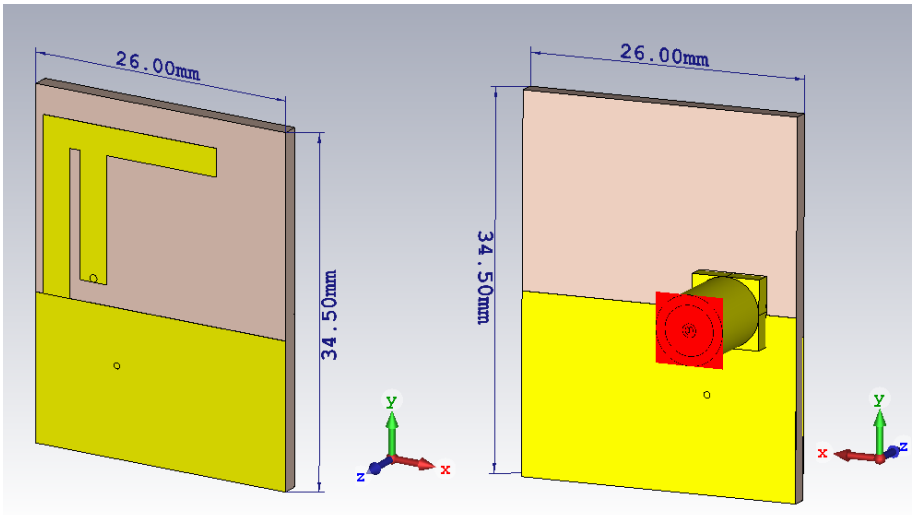

Figure 4.1: 3D front (left) and back (right) view of the designed PIFA.

The overall dimension of this antenna is 34.50x26.00x1.6 mm^3, which gives a radius of the smallest circle involving the antenna of 21.6 mm. This is a little bit above the maximum 19.5 mm determined by equation (3.2). Its S11 parameter in dB with 3 markers, one for the s-parameter at 2.45 GHz and the other two to display the bandwidth at -10 dB is displayed in figure 4.2.

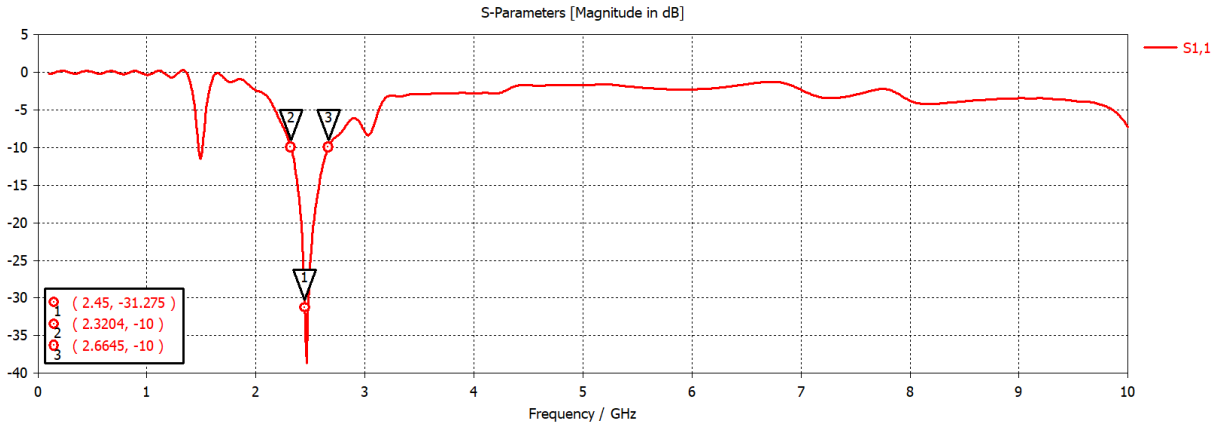

Figure 4.2: S11 of the designed PIFA.

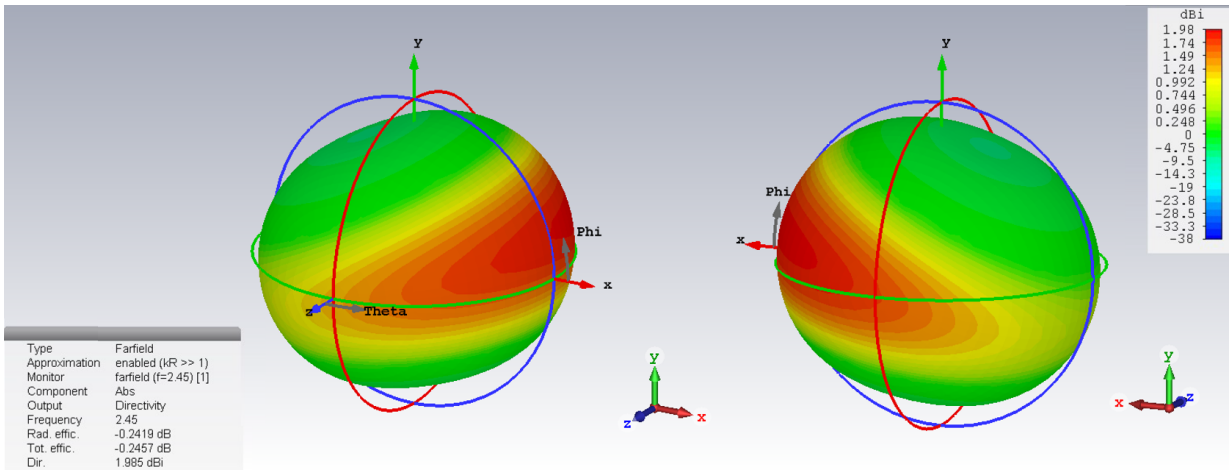

Figure 4.3: 3D front (left) and back (right) view of the radiation diagram of the designed PIFA.

Figure 4.3 shows the PIFA's three-dimensional radiation diagram where it can be seen that the designed antenna is not omnidirectional, but the difference between the highest gain factor point (in the centre of the most red pattern) and its antipodal point (assuming the radiation diagram to be a sphere this would be the opposite point through the centre) is of about 1 to 1.5 dB, so for smaller amplitude received signals this difference wouldn't be relevant. However, for high power applications that is not the case, for example, the difference between a received power of 0 dBm (1 mW) and 1.5 dBm (1.4 mW), isn't much but between 50 dBm (100 W) and 51.5 dBm (141 W) is very significant.

Next is the meander line antenna, whose 3D front and back view is displayed in figure 4.4.

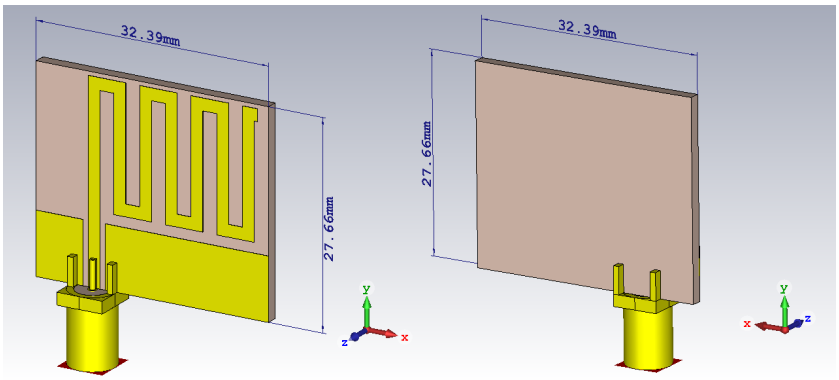

Figure 4.4: 3D front (left) and back (right) view of the designed meander line antenna.

The overall dimension of this antenna is 32.39x27.66x1.6 mm^3, which gives a radius of the smallest circle involving the antenna of 21.3 mm, which is above the smallest radius containing the whole antenna. However, the 32.39 mm dimension can be easily decreased without compromising the antenna's response too much and by decreasing only 5 mm, resulting in a 27.39x27.66x1.6 mm^3 the a would fall down to 19.46 mm, which is exactly at the limit required to be defined as a electrically small antenna.

Again with the same configuration of marker, figure 4.5 shows the S11 for the meander line antenna.

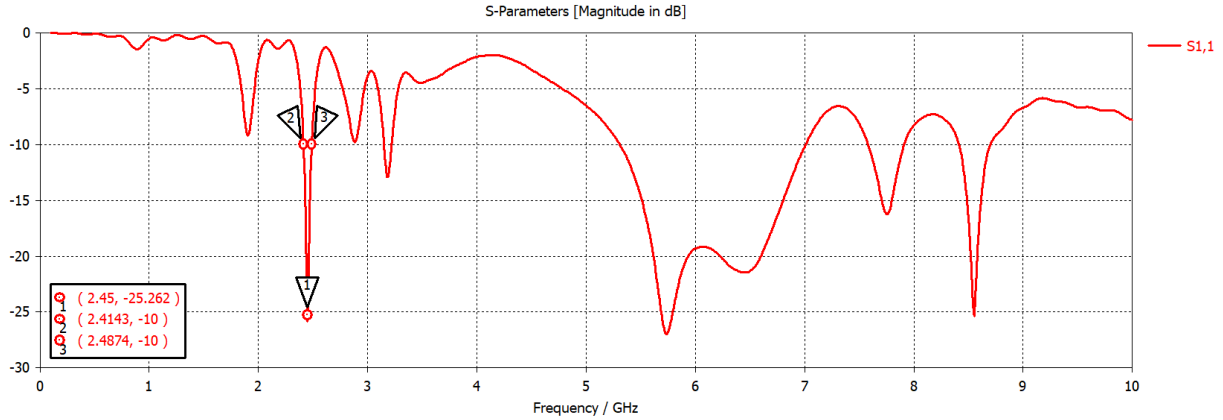

Figure 4.5: S11 of the designed meander line antenna.

The meander line antenna's radiation pattern is displayed bellow (Figure 4.6).

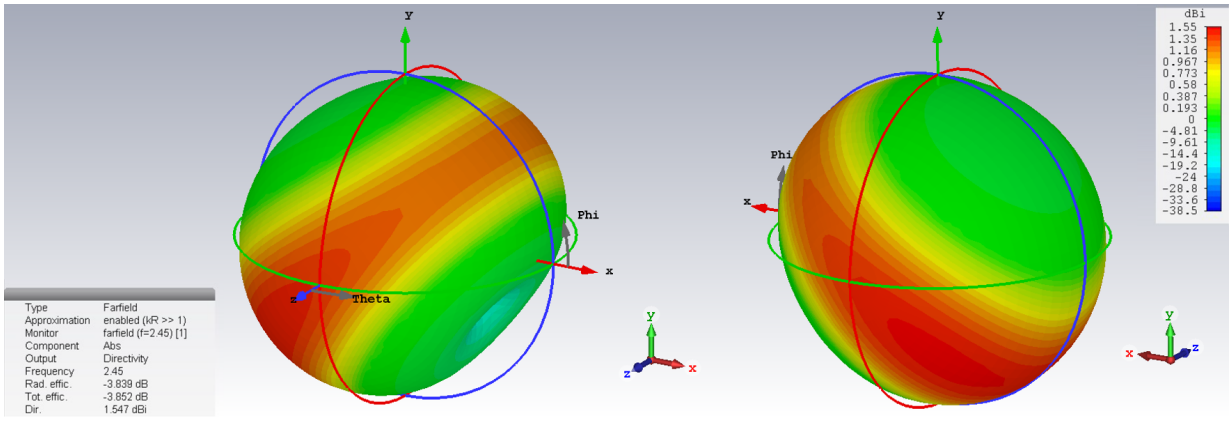

Figure 4.6: 3D front (left) and back (right) view of the radiation diagram of the designed meander linde antenna.

This radiation pattern is closer to a omnidirectional pattern with the referred difference, in the previous couple of antennas, of only approximately 0.5 dB.

For the next antenna, a patch antenna was designed resulting in the 3D view shown in figure 4.7.

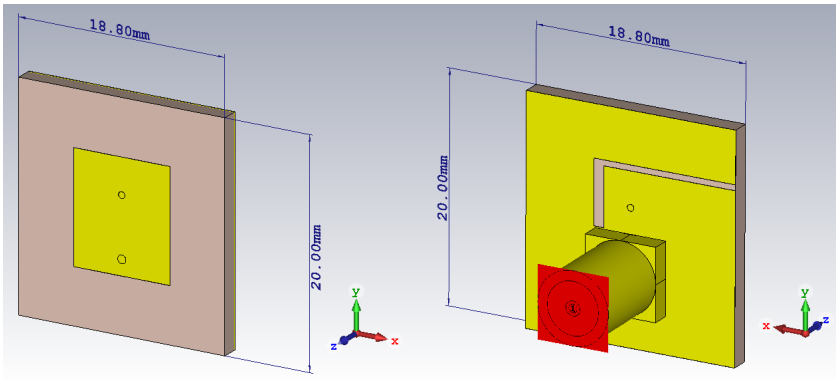

Figure 4.7: 3D front (left) and back (right) view of the designed patch antenna.

The overall dimension of this antenna is 20.00x18.80x1.6 mm^3, which gives a radius of the smallest circle involving the antenna of 13.7 mm, which is well bellow the 19.5 mm maximum and makes this a electrically small antenna. Followed by its S11 parameter in dB, with the same configuration of markers as the previous, which is shown in figure 4.8.

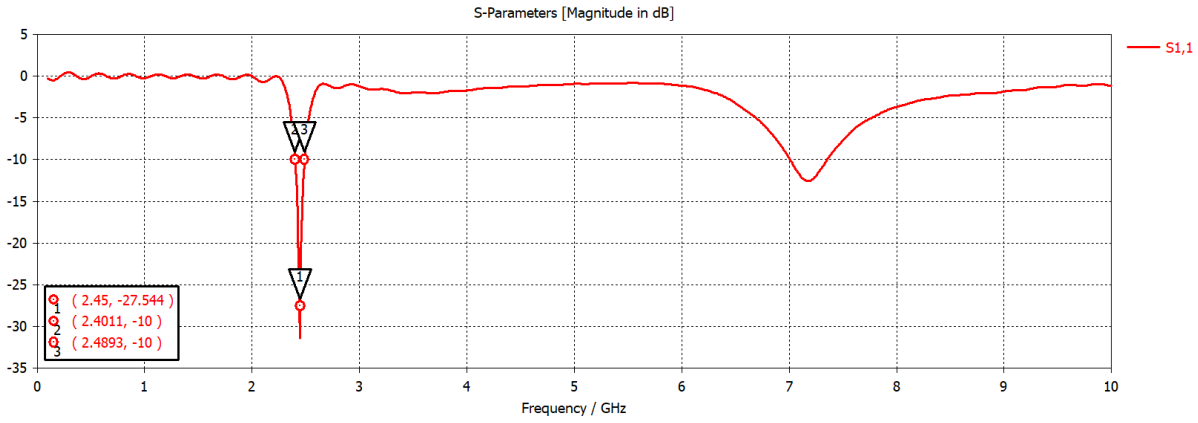

Figure 4.8: S11 of the designed patch antenna.

And its three-dimensional radiation pattern (Figure 4.9).

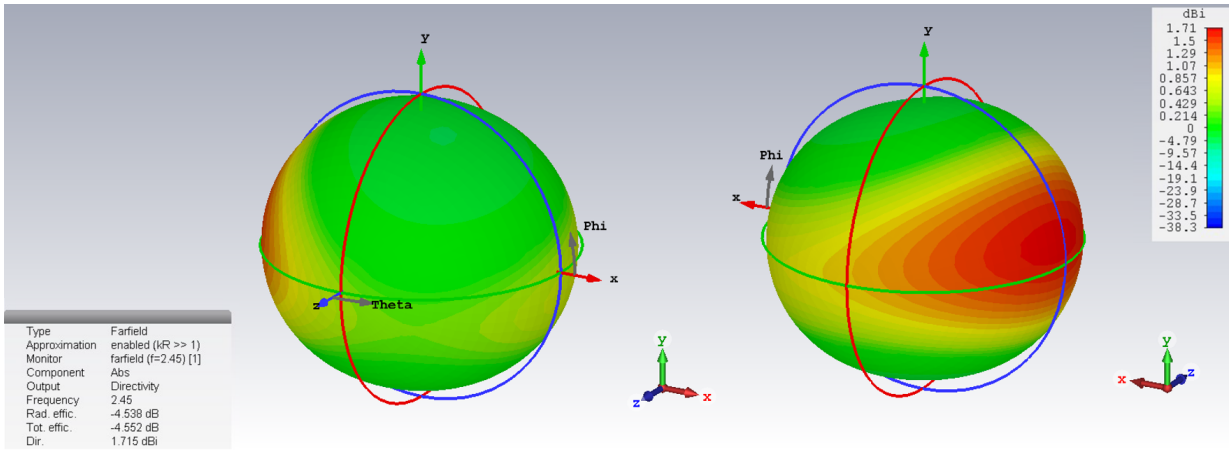

Figure 4.9: 3D front (left) and back (right) view of the radiation diagram of the designed patch antenna.

From this radiation pattern, it can be seen that the patch antenna is not completely omnidirectional, but, again, the variation of the omni-directivity is around 1.5 dB.

Moving on to the loaded monopole, figure 4.10, with a volume of 28.00x18.00x1.6 mm^3, which in turn results in a smallest circle radius of 16.6 mm, being then considered a electrically small antenna.

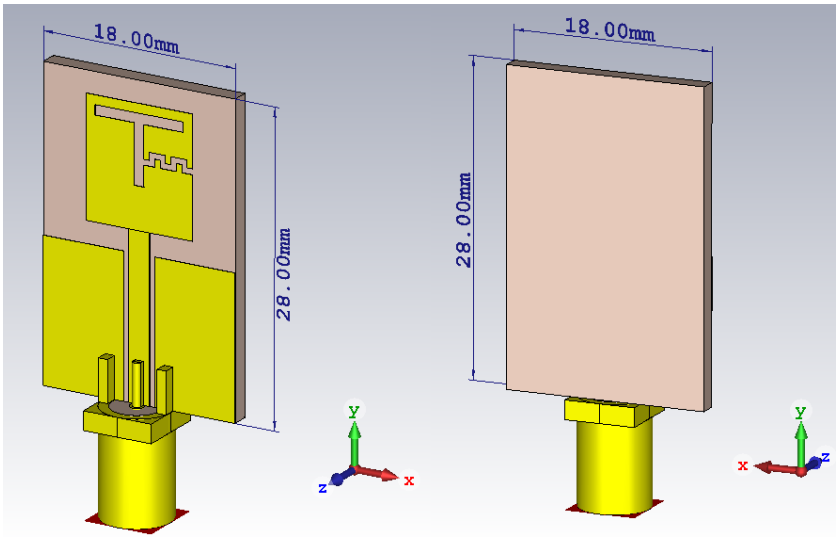

Figure 4.10: 3D front (left) and back (right) view of the designed loaded monopole.

The S-parameter of this monopole is displayed in figure 4.11 with the 3 markers like the previously displayed S11 parameters.

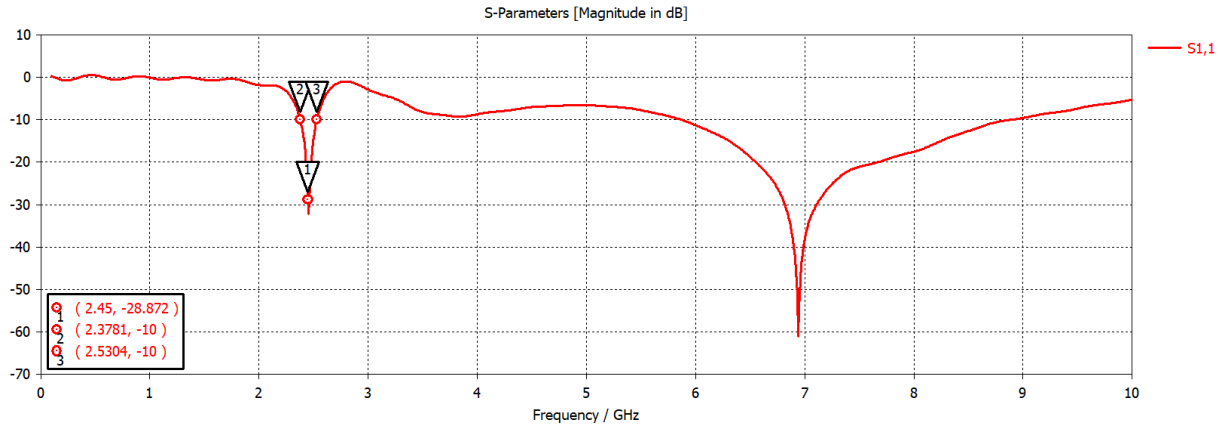

Figure 4.11: S11 of the designed loaded monopole.

Followed by the three dimensional radiation diagram, figure 4.12.

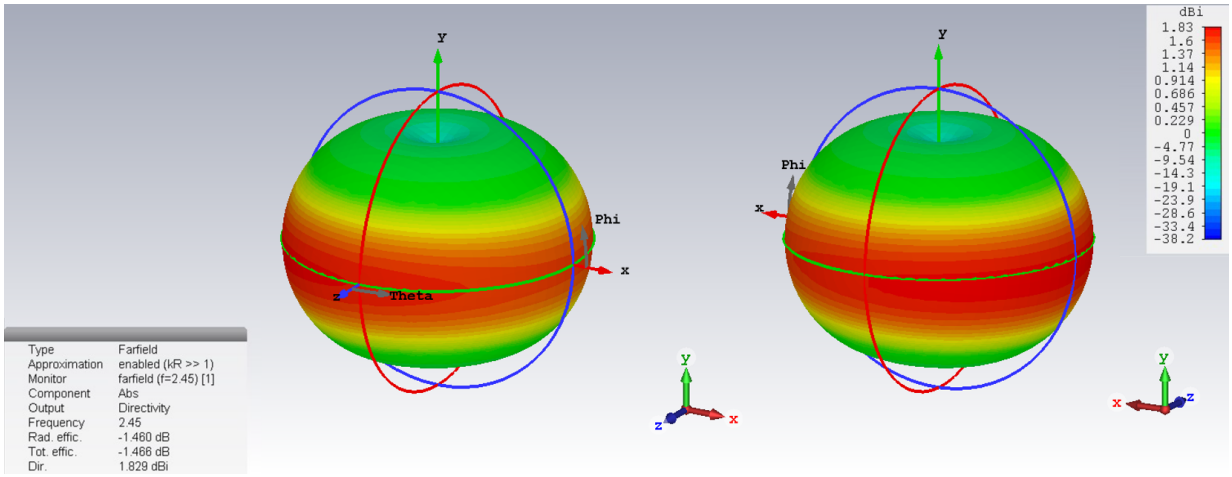

Figure 4.12: 3D front (left) and back (right) view of the radiation diagram of the designed loaded monopole.

This is clearly a omnidirectional pattern, with a difference between gain peak and its antipodal point of 0.2 dB. This antenna would be a good choice for a application that needed an omnidirectional pattern.

Last but not least, is the CSRR loaded antenna with a CSRR and a capacitive flare, figure 4.13.

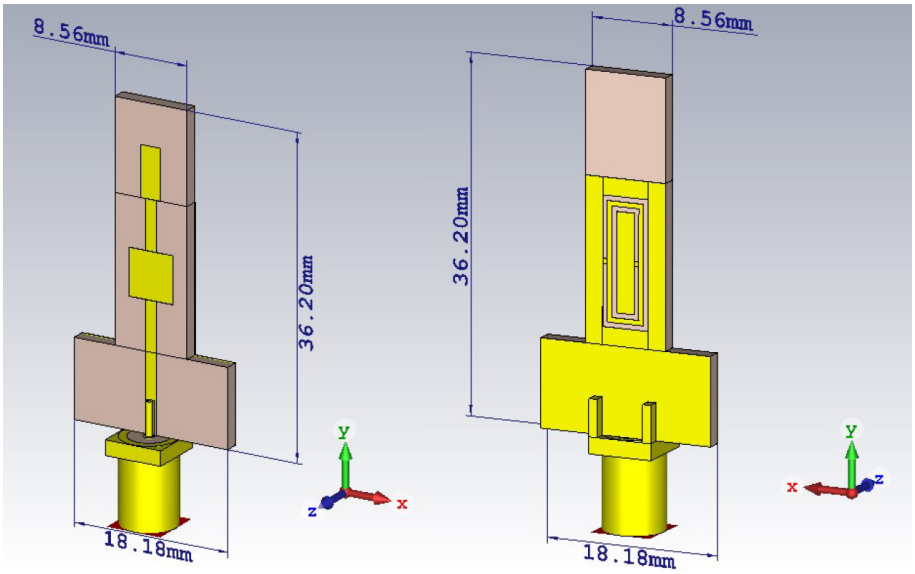

Figure 4.13: 3D front (left) and back (right) view of the designed CSRR loaded antenna.

This design is not a square or a rectangle, so the smallest circle involving the whole antenna will not be exactly at the middle of the 18.18x36.20x1.6 mm^3 surface, since the antenna has a narrower part with 8.56 mm width, but, assuming the first, the radius is 20.3 mm which is just above the 19.5 mm limit.

The CSRR loaded antenna's S11 parameter is presented in figure 4.14.

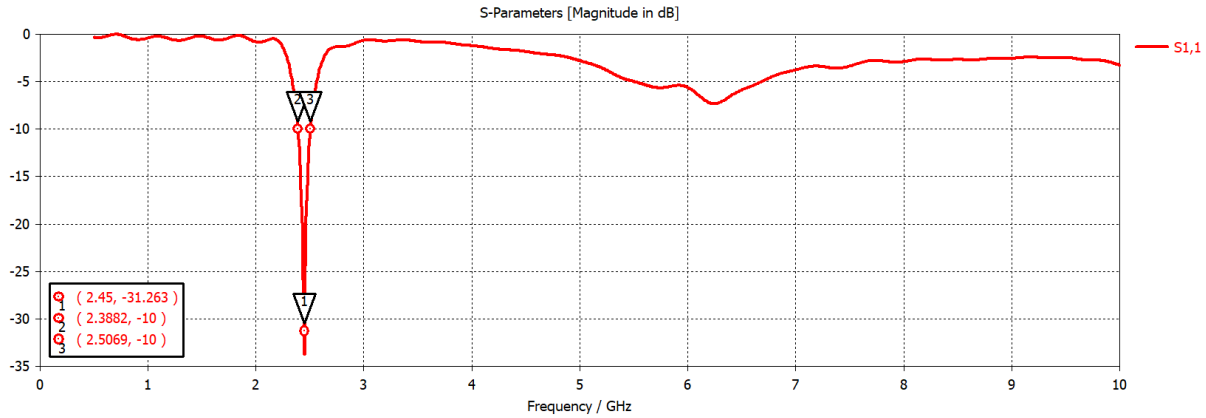

Figure 4.14: S11 of the designed CSRR loaded antenna.

Finally, its three dimensional radiation pattern (Figure 4.15).

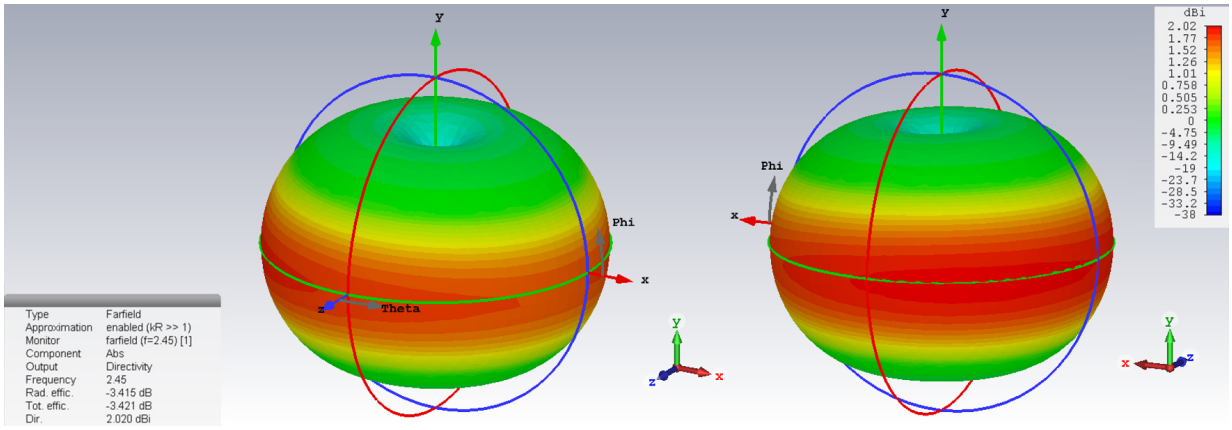

Figure 4.15: 3D front (left) and back (right) view of the radiation diagram of the designed CSRR loaded antenna.

This CSRR loaded antenna is almost completely symmetric and so, as expected, the radiation pattern is omnidirectional (with just a slight variation of 0.5 dB). The only asymmetric component is the CSRR, but, changing it, changes the S11 parameter and moves the resonance to another frequency, so this issue would have to be carefully approached.

Table 4.1 organises the impedance bandwidth at -10 dB, with lower and higher limits, and S11 level at 2.45 GHz to simplify the analysis. The patch and meander line antennas have lower bandwidths and the PIFA, although having a good bandwidth considering the magnetron's variations in frequency, doesn't have a good radiation pattern. The two best choices would be the loaded monopole and the CSRR loaded antenna whose bandwidths are, approximately, 150 MHz and 120 MHz, respectively, and around -30 dB S11 parameter.

Antenna	Range (GHz)	Bandwidth (MHz / %)	S11 (dB)
PIFA	2.320 - 2.664	344 / 13.8	-31.28
Meander Line	2.414 - 2.487	73 / 3.0	-25.26
Patch	2.401 - 2.489	88 / 3.6	-27.54
Loaded Monopole	2.378 - 2.530	152 / 6.2	-28.87
CSRR loaded	2.388 - 2.507	119 / 4.9	-31.26

Table 4.1: Bandwidth at -10 dB and S11 (dB) of resonance at 2.45 GHz comparison.

The bandwidth percentages are only calculated for resonances that include 2.45 GHz.

Although all these antennas could be used in 2.4 ± 0.1 GHz applications, since the experiments conducted in this dissertation are subjected to extremely high power signal, a simple $\lambda/4$ with 50 Ω equivalent width for 2.45 GHz monopole was designed. This antenna was not optimised, to relax the system and prevent the overpowering of the RF to DC converter.

This monopole's 3D view can be seen in figure 4.16.

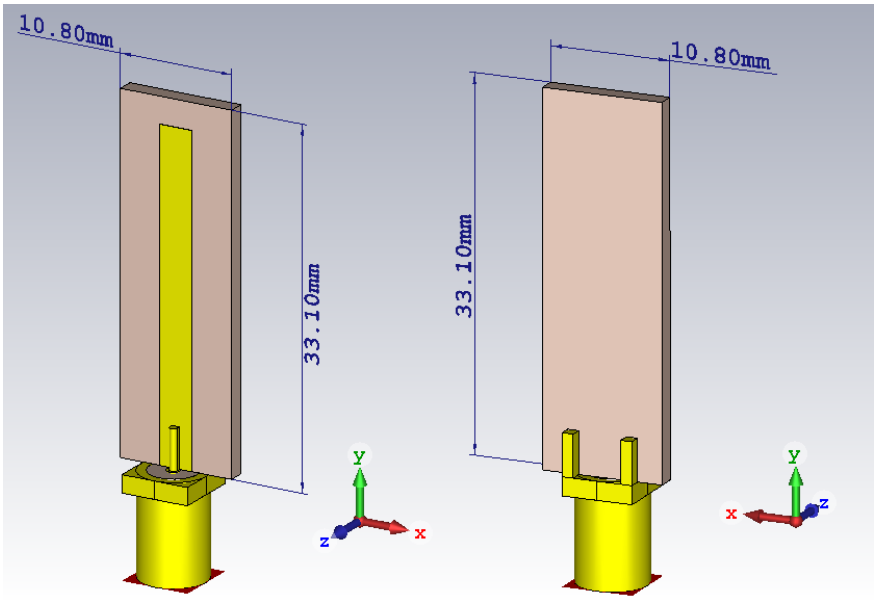

Figure 4.16: 3D front (left) and back (right) view of the designed monopole.

Moreover, in figure 4.17, the not adapted S11 parameter.

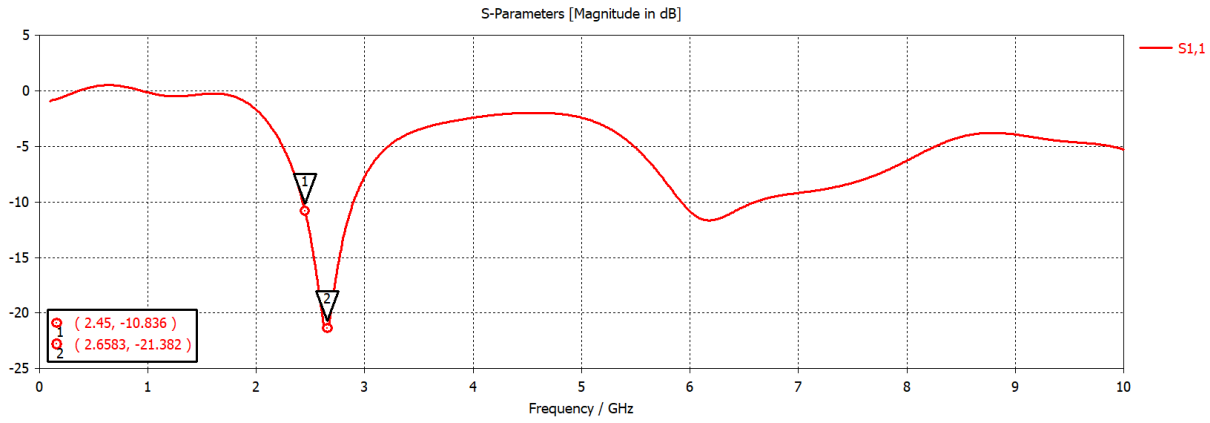

Figure 4.17: S11 of the designed monopole.

Finally, the monopole three dimensional radiation pattern in figure 4.18.

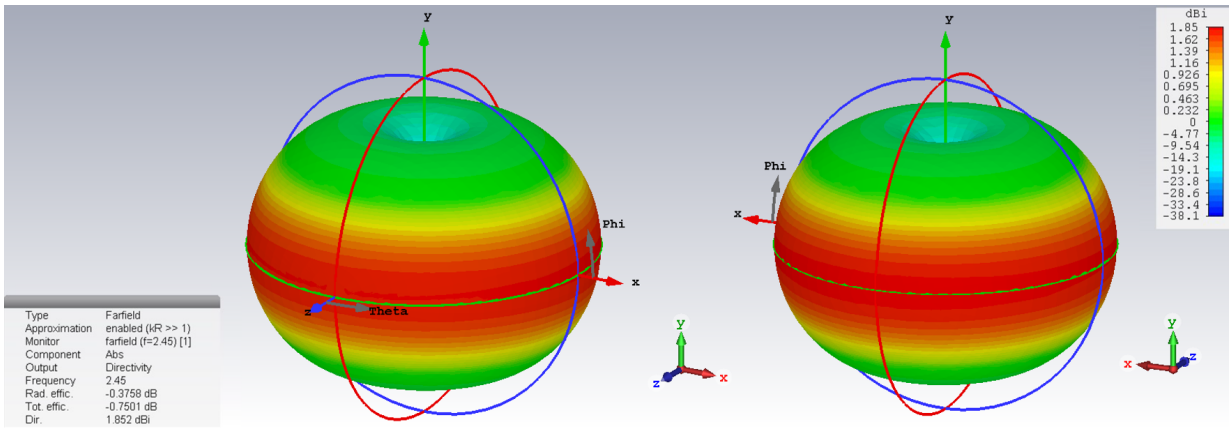

Figure 4.18: 3D front (left) and back (right) view of the radiation diagram of the designed monopole.

As expected, this antenna has a completely omnidirectional pattern. The monopole's dimensions are 33.10x10.80x1.6 mm^3, which results in a radius, of the smallest circle, of 17.4 mm ($<$ 19.5 mm) making it a electrically small antenna.

4.1.2 Printed and Measured

Figure 4.19: Printed monopole antenna front and back view.

The monopole antenna was printed and measured. Upon its measurement, the S parameter wasn't very stable. This might be due to the back not having any copper, as it can be seen in figure 4.19, which hinders the welding of the SubMiniature version A (SMA) connector to the Printed Circuit Board (PCB). To fix this, a epoxi Araldite glue was used to further roughen up the connection between the SMA connector and the monopole, figure 4.20.

Figure 4.20: Glue roughening up the connection between the connector and the monopole.

With that in mind, figure 4.21 shows the S parameter exported from CST compared with the measured S parameter.

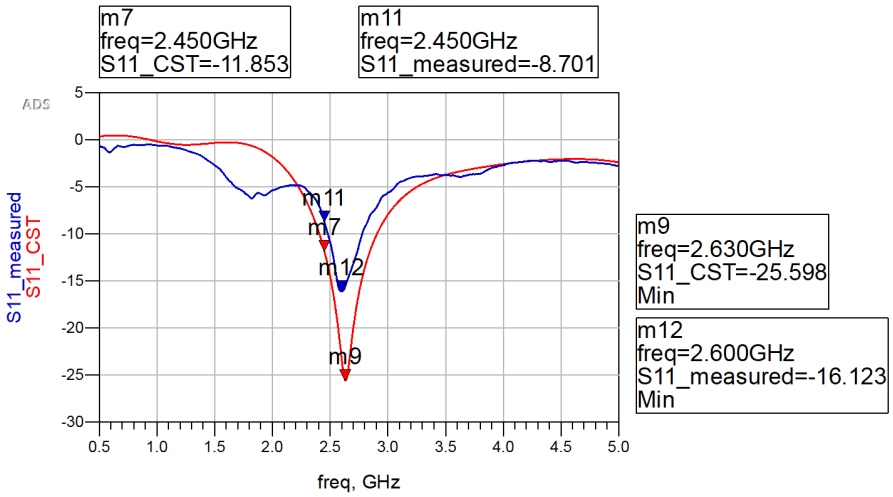

Figure 4.21: S11 from CST compared with measured S11 of the monopole.

4.2 RF-DC Converter

For the conversion of the RF signal to a DC voltage, the configurations mentioned in chapter 3 were designed and simulated using ADS software. All simulated circuits started with an ideal equivalent, with ideal components, then with ideal lines and, finally, with microstrip lines. The Harmonic Balance (HB) and the Large Signal S Parameter (LSSP) simulation controllers were used. The HB to simulate the output voltage and the input power source and the LSSP to simulate the S parameters for large signals, since this circuit will have to be capable of handling extremely high levels of power.

The input power (pin) displayed in the simulated and measured results is in dBm, the output voltage (Vout) is in volts, V, and the efficiency is in percentage, %.

4.2.1 Diode Rectifier Designs

For the first experiment, three configuration of the Dickson multiplier were designed. The difference between them, apart from the lines' lengths and widths, is how the feedback is done. In the first configuration, the feedback is done by a shunt diode, in the second by an inductor and lastly by a short stub.

The schematic of the converter with a shunt diode is displayed in figure 4.22.

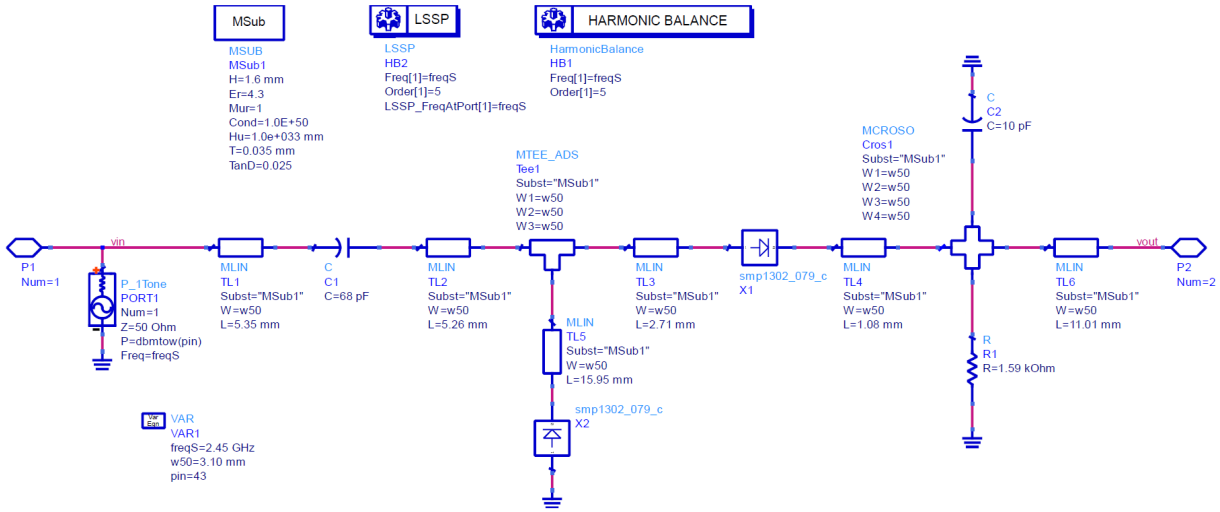

Figure 4.22: Schematic of the converter with a shunt diode feedback.

In figure 4.23 is represented the schematic used for the converter with a DC feed inductor.

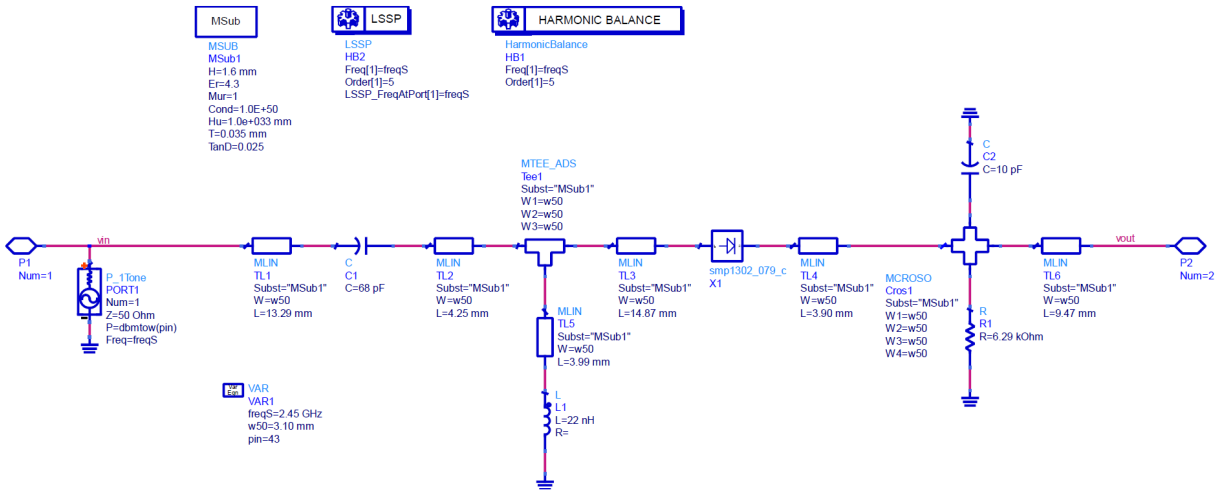

Figure 4.23: Schematic of the converter with a DC feed inductor feedback.

Finally, the schematic showing the circuit with a short stub, figure 4.24.

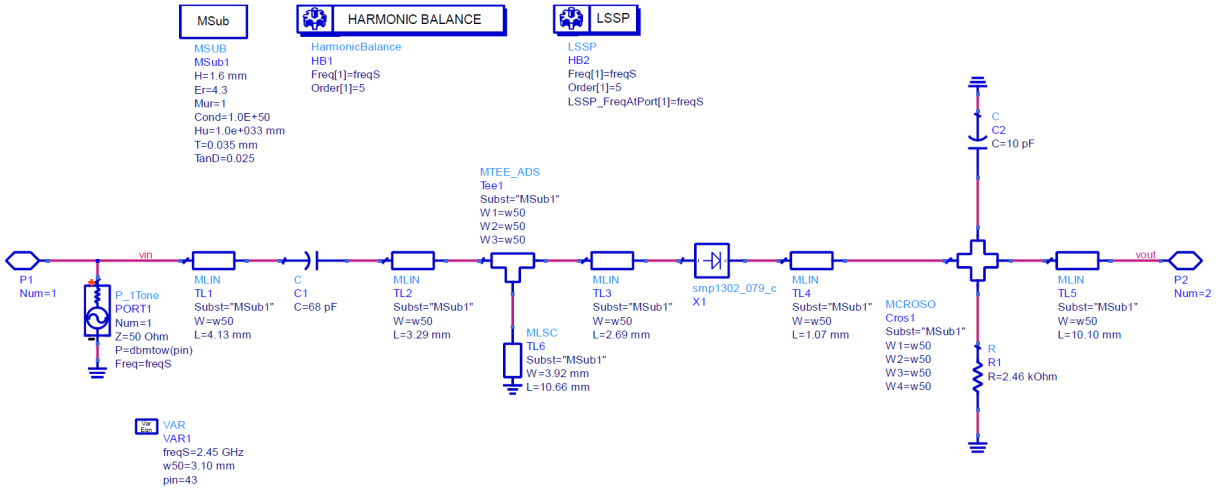

Figure 4.24: Schematic of the converter with a short stub as the feedback.

Figures 4.25 and 4.26 show the S11 parameter and the efficiency and output voltage as a function of input power for each circuit. All the graphics start with 20 dBm input power and go up to the maximum power level that, according to simulation, doesn't exceed the "explosion current".

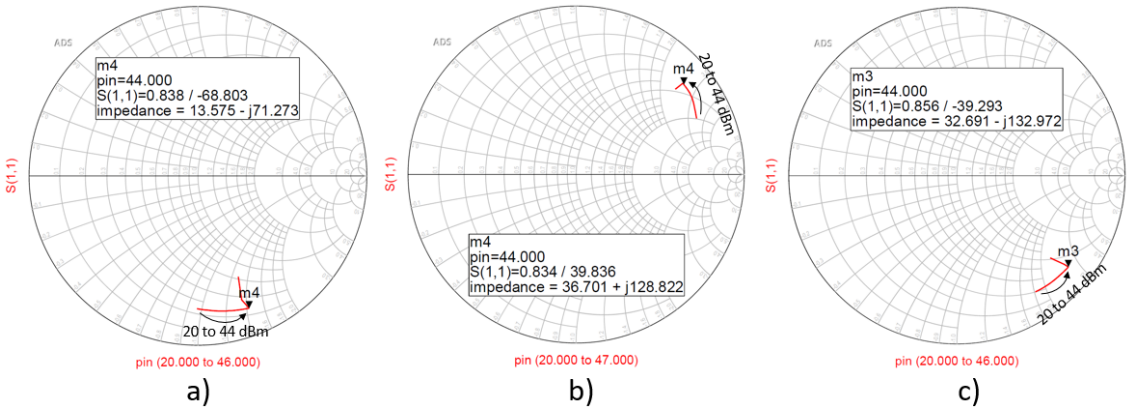

Figure 4.25: S11 parameter of the RF-DC circuit with a) short stub, b) shunt diode and c) inductor feedback.

The markers are placed at the turning point between input power that produces low reverse voltage and reverse voltage approaching the breakdown voltage.

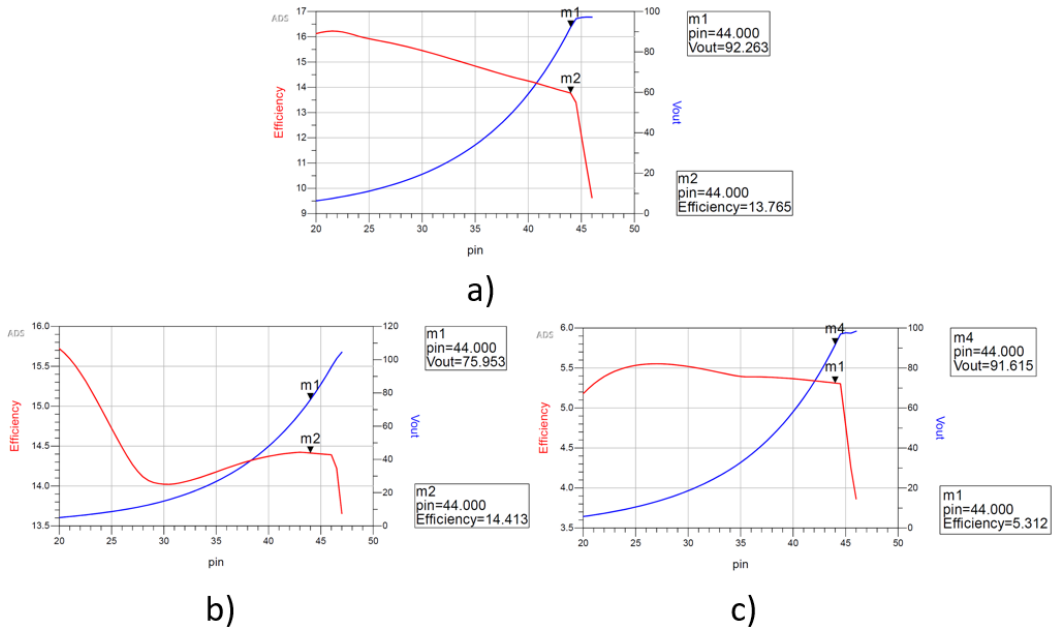

Figure 4.26: Efficiency and output voltage of the RF-DC circuit with a) short stub, b) shunt diode and c) inductor feedback.

Since the goal for energy-harvesting circuits is to have high efficiency, a rectenna design combining the antenna and the rectifying circuit was tested. Figure 4.27 shows the plastic structure used to hold the PCB's with the monopole antenna and the RF to DC converter in the middle of the microwave oven. The structures involving the circuits are made of plastic and don't shield the circuit from electromagnetic waves.

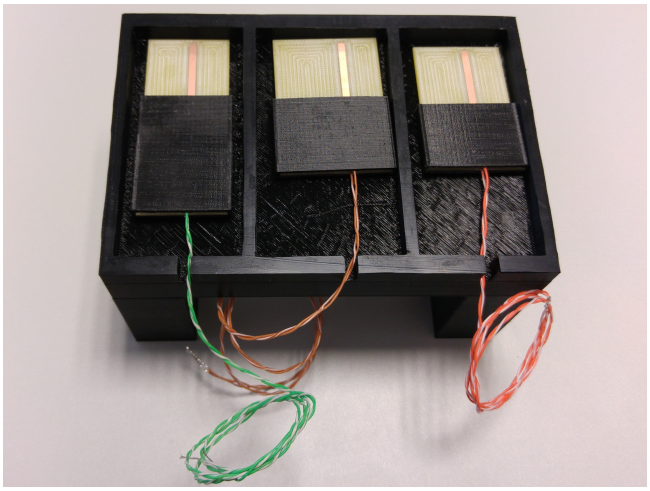

Figure 4.27: Printed monopole and converter pairs for the first experiment.

In the setup for the first experiment, figure 4.28, the turntable was removed and a glass of water was put inside with the circuits.

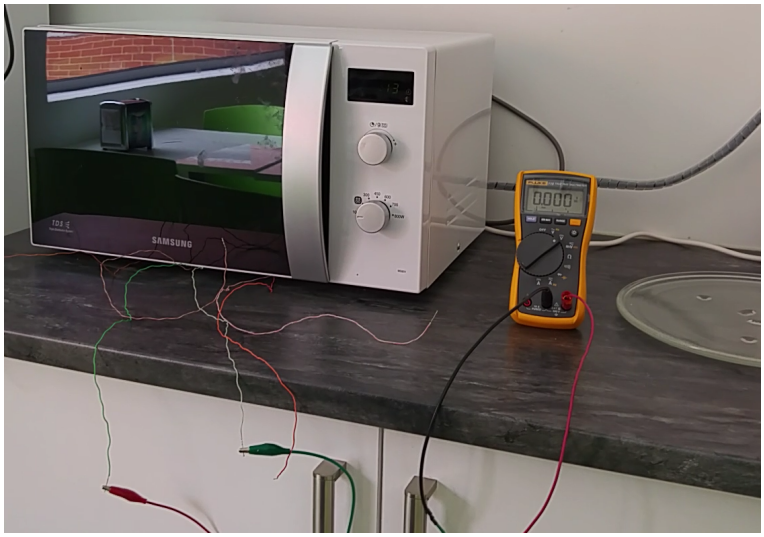

Figure 4.28: Setup of the first experiment.

The voltage meter measured a small voltage of 0.016 V and rapidly raised to 0.991 V, figure 4.29.

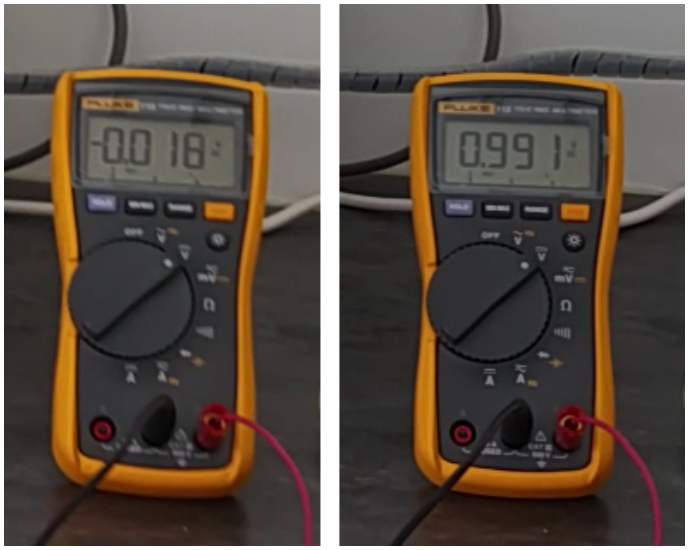

Figure 4.29: Voltage levels of the first experiment.

After that, a second attempt was tried, but the circuits were already burnt, figure 4.30.

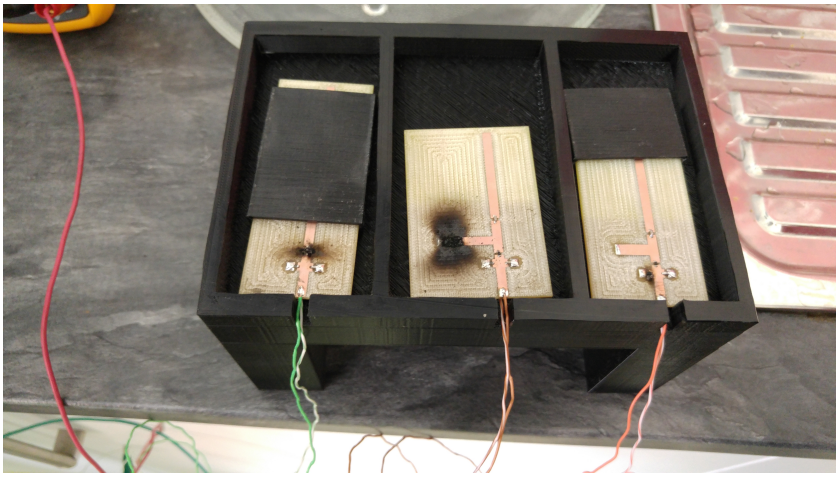

Figure 4.30: Result of the first experiment.

A picture of the circuits before testing wasn't taken but, comparing figure 4.30 with the schematics previously presented, each circuit combined with the monopole antenna can be identified. From the left to the right are the inductor, shunt diode and short stub feedback circuits.

By analysing the results of each circuit board, several aspects can be concluded. The configuration with a shunt diode (middle) is the less reliable, since the shunt component will have to handle high levels of current and, even though these diodes can take high levels of reverse voltage, their maximum forward current is still low. The configuration with a short stub (right) worked better, but the output resistor was too low and burned. For the next designs, it's advised to choose higher values of the output resistor. The configuration with a DC feed inductor had a higher valued resistor but the diode burned. With these results, it is clear that alternative ways for current flow, specially in the rectifier diode zone, should be added. Also, mismatching the circuit, in order to lower the power delivered to the non-linear element, can help relax the rectifiers performance.

4.2.2 Alternative Diode Rectifiers

The optimisation goals are now different. First, every lumped element's maximum ratings must not be exceeded, then the output DC voltage must be guaranteed and, finally, the input impedance, that even though it should be mismatched to relax the lumped elements, can be optimised without neglecting the previous goals. This can easily be done by setting each goal's weight according to their priority.

One of the RF to DC rectifiers designed has an inductor feed (Figure 4.31) and the other has a short stub feed (Figure 4.32).

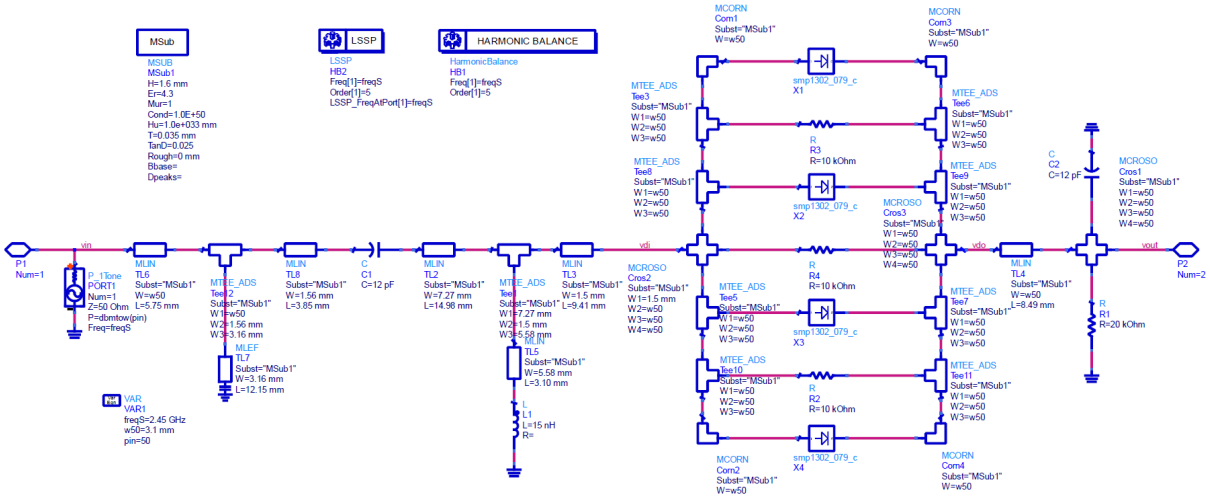

Figure 4.31: Schematic of the alternative converter with an inductor feed.

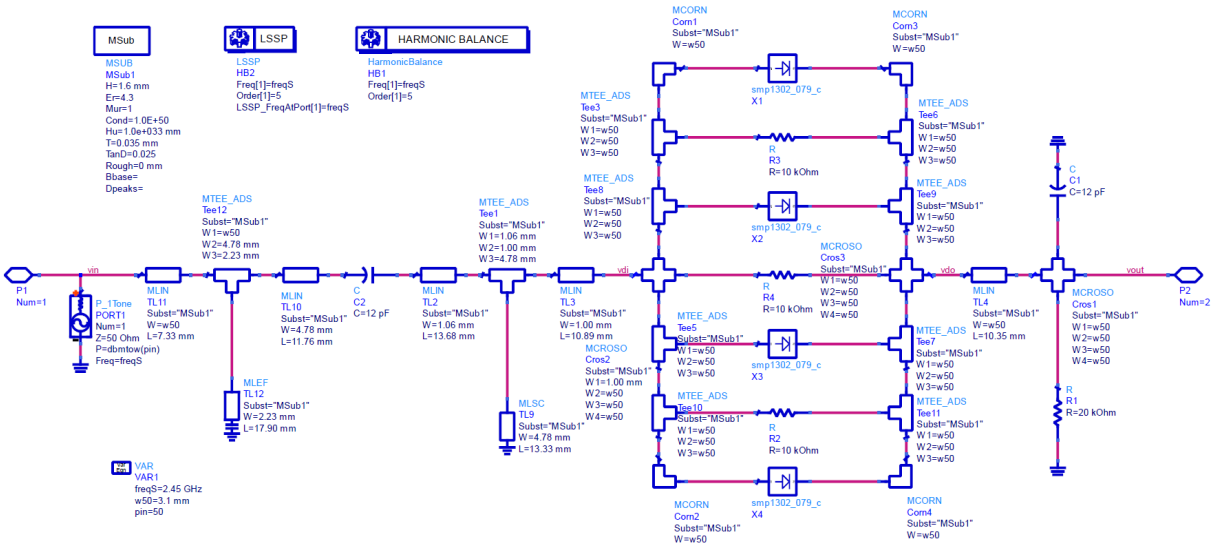

Figure 4.32: Schematic of the alternative converter with a short stub feed.

The efficiency and output voltage of the a) inductor and b) short stub rectifiers are shown in figure 4.33. An improvement in input power handling can be clearly seen, but the efficiency decreased comparing to the first designed circuits.

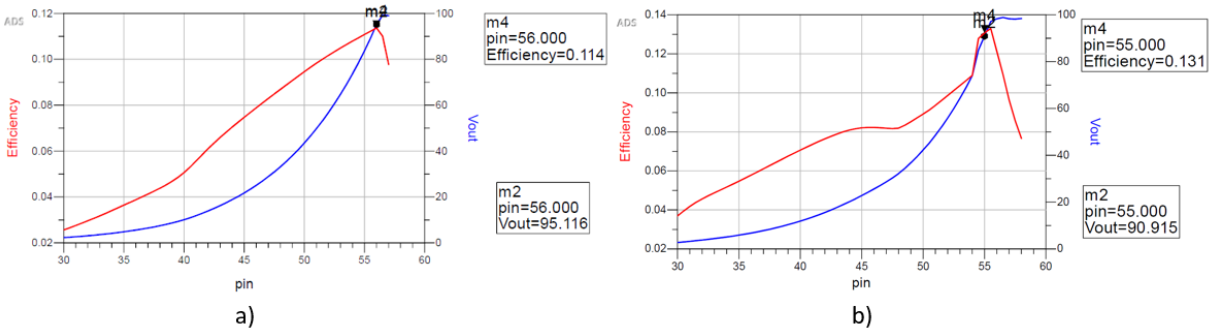

Figure 4.33: Efficiency and output voltage of the alternative RF-DC circuit with a) inductor, b) short stub feedback.

Figure 4.34 shows the input impedance of the new rectifiers which have a lower variation with input power than the previous rectifiers. This might be due to the resistors in parallel with the diodes.

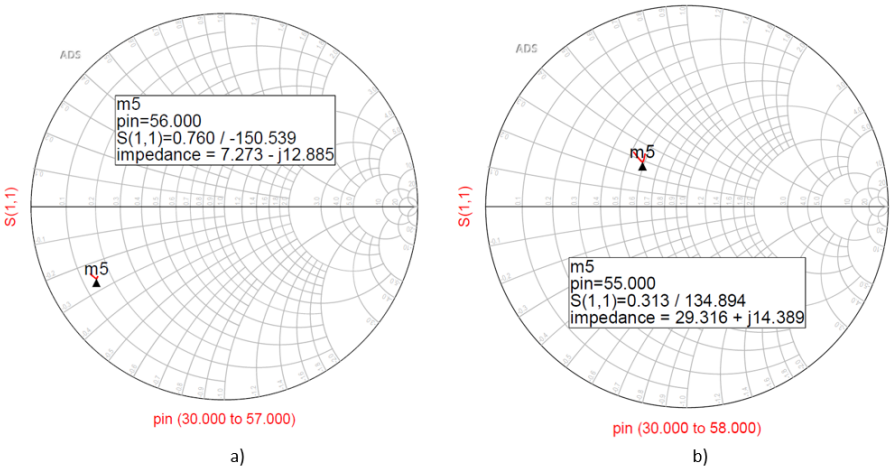

Figure 4.34: Reflection coefficient of the alternative RF-DC circuit with a) inductor, b) short stub feedback.

In order to test these new rectifying circuits, before putting them inside the microwave oven, they were printed separately from the monopole antenna. To set up this experiment, a high output power handling amplifier, a Vector Signal Generator (VSG) and a set of isolators were required. The power amplifier used was the Mini-Circuits' high power amplifier ZHL-30W-252+. The Rohde&Schwarz SMJ100A VSG was connected to a Agilent's N1913A EPM Series Power Meter to check, with precision, the VSG's output power so that the power amplifier's maximum output power would not be exceeded (Figure 4.35 left).

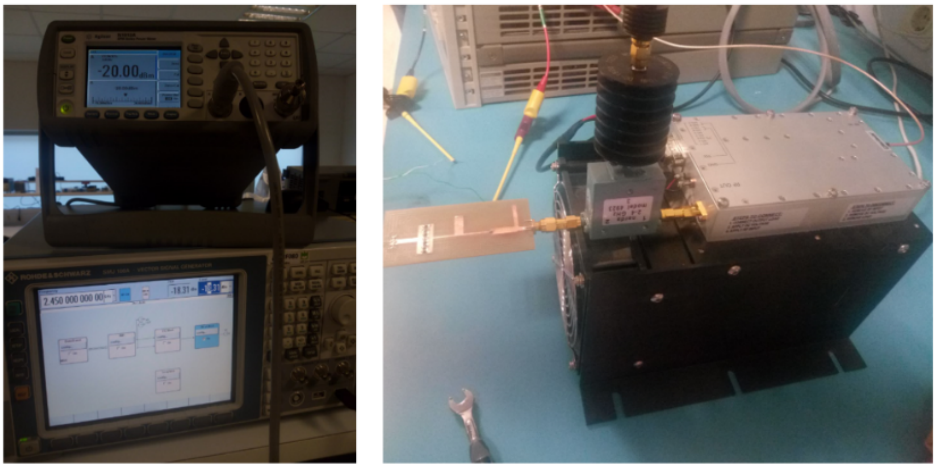

Figure 4.35: On the left, a power meter checking the VSG's output power and, on the right, the setup for driving the designed converter.

In figure 4.35, on the right, the power amplifier is shown, follower by a L3 Narda-MITEQ's isolator model 4923 and the RF to DC converter. At approximately 40 dBm at the converter's input, the output voltage measured on a multimeter was 7 mV for the converter with short stub and 2 mV for the converter with inductor, both with SMP1302 diodes. The same circuits, with SMP1304 diodes didn't give any voltage, because, as it will be demonstrated later, they give lower output voltages, probably due to having higher series resistance, R_S.

4.2.3 Transistor Design

With high power signal, the circuitry lines usually need to be bigger (wider or longer) and, since the goal is to put the power probe inside the microwave oven, small size is desired. An output capacitor was also added to improve the filtering aspect of the RF choke. After some experiments on different matching networks, both at the input and at the gate, the circuit represented in figure 4.36 was designed. The design goals were similar to the previously mentioned, lumped components maximum ratings must not be exceeded, output DC voltage must be guaranteed and an additional goal to set the transistor's drain-source current and voltage to levels bellow their maximum ratings.

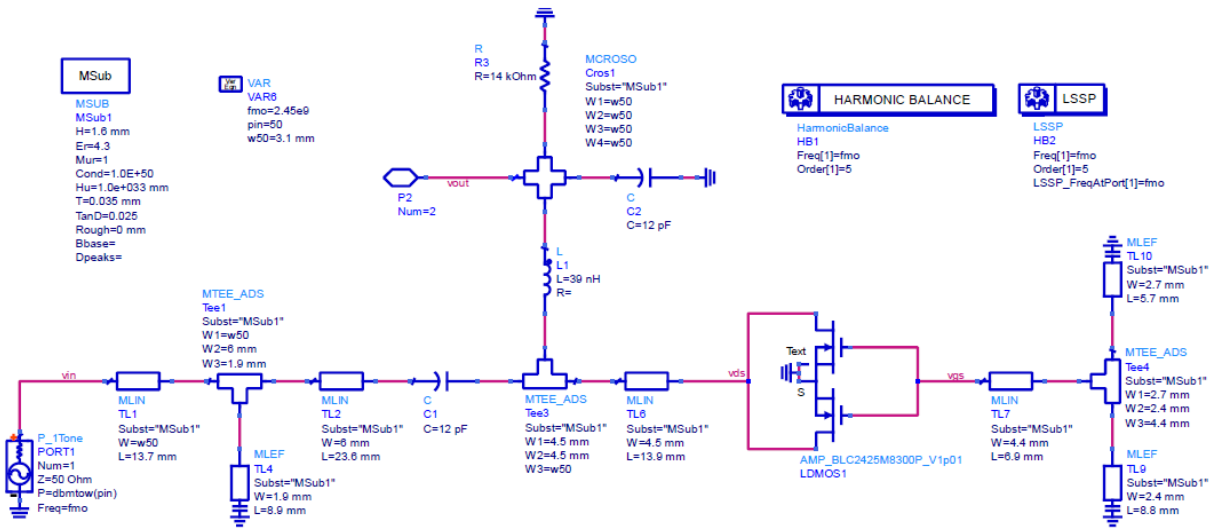

Figure 4.36: Designed transistor based rectifier.

The efficiency and output DC voltage are displayed in figure 4.37. The input impedance in figure 4.38.

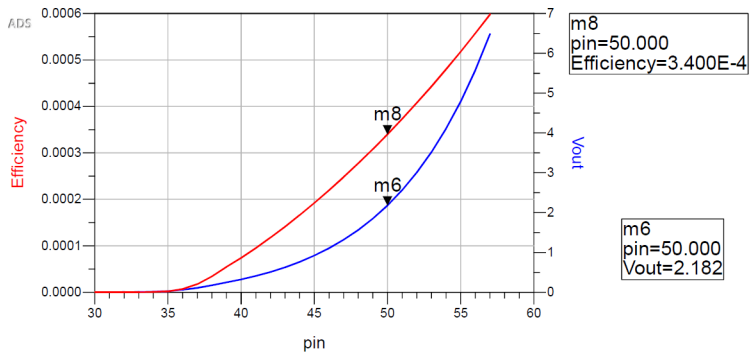

Figure 4.37: Efficiency and output voltage of the designed transistor based rectifier.

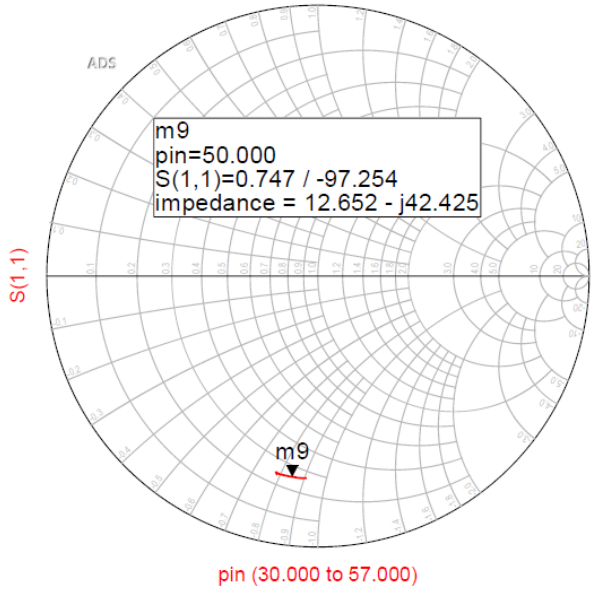

Figure 4.38: Input impedance of the designed transistor based rectifier.

High reflection coefficient and high output load resistance are the two main contributors to the low levels of efficiency, but reducing both would stress the circuit and the maximum ratings of the components could be exceeded.

4.2.4 Microwave Oven Tests

Three different topologies were designed. The diode-based rectifier with an inductor, figure 4.39, with a short stub, figure 4.40, and the transistor-based rectifying circuit, figure 4.41.

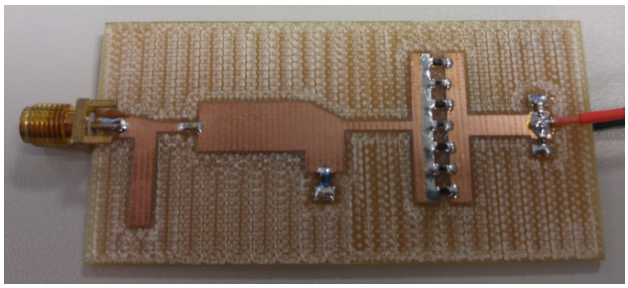

Figure 4.39: Printed diode-based rectifier with an inductor.

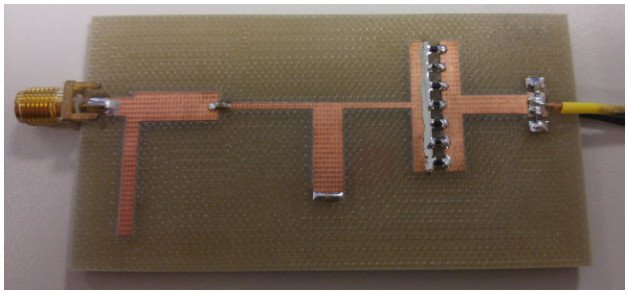

Figure 4.40: Printed diode-based rectifier with a short stub.

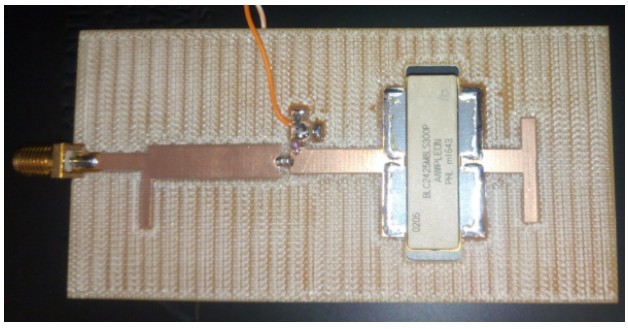

Figure 4.41: Printed transistor-based rectifier.

The diode rectifier with an inductor, together with the monopole antenna, was inserted into a 3D printed plastic box, figure 4.42, which was covered by a ECCOSORB LS absorbent, figure 4.43, and then involved in aluminium foil, 4.44.

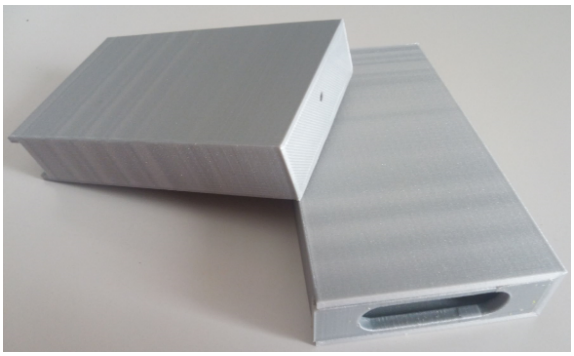

Figure 4.42: 3D printed plastic box.

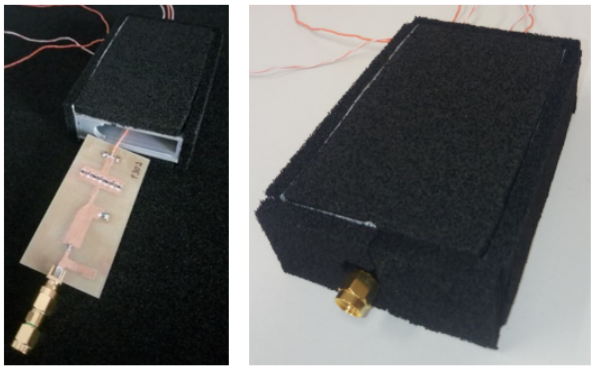

Figure 4.43: 3D printed plastic box involved in a absorbent.

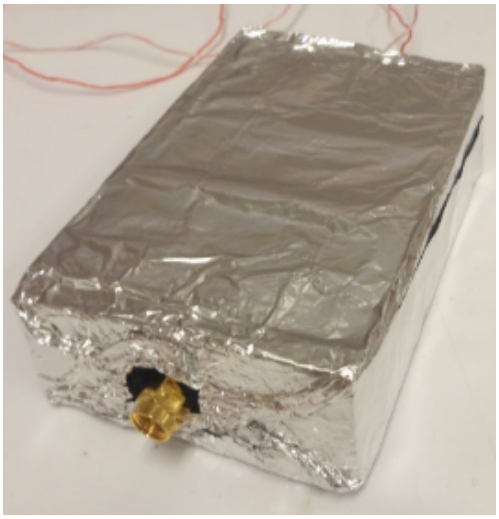

Figure 4.44: 3D printed plastic box involved in a absorbent involved in aluminium foil.

Inside the microwave oven (with two glasses of water), this setup actually gave a decent output voltage, but there were some sparks. The circuitry was intact, so the problem wasn't there. The sparks were actually caused by the combination of the absorbent sheet and the aluminium. Figure 4.44 shows the aluminium covering almost all the absorbent, but the tiny exposed absorbent did absorb some radiation and heated up, which, in turn, heated the aluminium. The sparks seen were around the input and might have been caused by heated up aluminium or arcs between the aluminium and the ground of the male-male coaxial adaptor. Also, a tiny spark on the back that justifies the slightly melted DC electric cables.

With that in mind, another isolating setup was attempted. In this case, an isolating tape was placed around the SMA adaptor, figure 4.45. Since the absorbent was heating up, the author opted not to use it and use only the aluminium tape/foil.

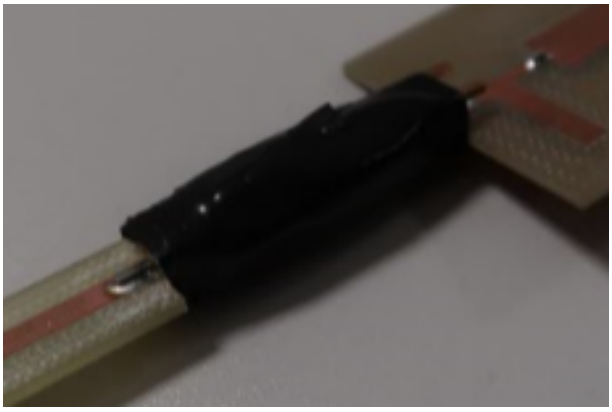

Figure 4.45: Isolating tape around coaxial adaptor.

On this experiment, the author forgot to turn down the wattage and, so, the first three runs were done with a 800 W radiating signal. Luckily, the antenna was placed in a null zone which, as explained in section 2.1.1, is a zone in the three-dimensional standing wave, that is formed inside the ovens cavity, where the power level is at its lowest. At 800 W, the antenna was always in the same position and the oven was turned on for 10 seconds with 3, 2 and 1 glasses of water. For 100 W, that first two trials had 3 and 2 glasses, but the voltage with 2 glasses remained at 0 mV, so a different position was attempted and the output voltage was 40 mV, which proves that the amount of power is lower in that null point. It should also be noted that the experiments with 3 glasses had one of the glasses right bellow the monopole antenna. This experiment also proves another aspect of

the electromagnetic field which is its response to load. Varying the amount of glasses of water in the cavity is the same as changing the load. The more water, the higher the load, the lower the available power delivered to the food, or in this case to the power probe.

Power	800 W			100 W		
Nº of Glasses	3	2	1	3	2	2
Output Voltage (mV)	0	7	21	0	0	40

Table 4.2: Output voltage levels depending on number of water glasses and position

The second attempt tested the diode-based rectifier with an inductor and the transistor-based rectifier. The diode power converter, in four different positions, gave output DC voltage levels of 0, 5, 17 and 65 mV and the transistor converter levels of 180, 330, 980 and 1280 mV, which clearly shows the power dependence of location and confirms the standing wave pattern. Both in this and in the previous experiment, there were no sparks and the rectenna elements remained operational, i.e. the circuits can handle high power levels and the shield effectively protects the circuitry from radiating power.

The next experiment compared equal topologies using the RF to DC converters, with a short stub, with both diodes, four SMP1302 in one and four SMP1304 in the other. The SMP1302 converter, in four different positions, reached output voltage levels of 4, 14, 42 and 75 mV, whereas the SMP1304 converter only reached 0, 1, 3 and 6 mV. This might be due to the SMP1304 having higher series resistance. However, there is another aspect that should be taken into account. Comparing the simulated and measured results, the diode-based rectifiers have much lower measured output voltages than those simulated. This might be due to the diode model and the ideal resistors in between them. Nevertheless, a good scope of output voltage is achieved in the SMP1302 rectifiers. This difference, between simulated and tested, does not happen with the transistor, which supports the fact that a good model is required in order to have a good agreement between simulated and measured results.

Finally, a test comparing the three different topologies in four different positions with two glasses of water (one in the far left corner of the cavity and another in the right corner near the door) was conducted. Table 4.3 shows the different DC voltages measured in the multimeter, figure 4.46.

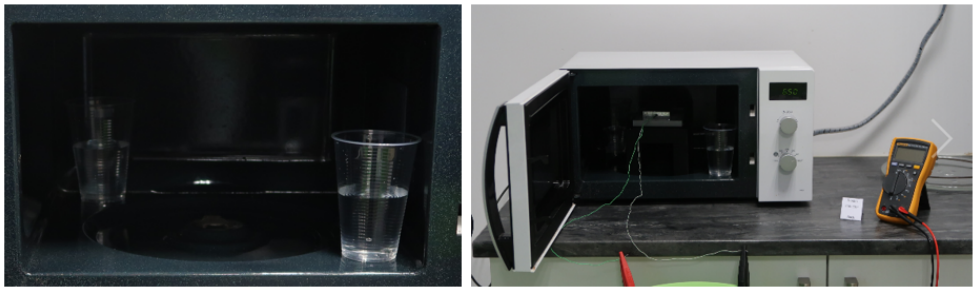

Figure 4.46: Four position test setup.

Position	Diode Rectifier Inductor (mV)	Diode Rectifier Short Stub (mV)	Transistor Rectifier (mV)
Back	17	5	120
Left	19	80	1100
Right	65	39	430
Door	32	28	490

Table 4.3: DC voltage levels comparison.

The variations in position clearly give different output voltages which validate the standing wave pattern. Other aspects, like the orientation of the aluminium foil structure and the different reflection coefficients, change the electromagnetic field inside the cavity, so a perfect comparison between the three topologies is very difficult. However, the diode-based rectifiers showed farely constant output voltage levels, whereas the transistor-based rectifier showed the rising and decreasing of the power delivered by the magnetron, which suggests a high precision in comparison with the diode-based rectifying circuits.

The charts in figures 4.47, 4.48 and 4.49 provide a visual representation of the voltage levels inside the microwave oven. The monopole was at, approximately, 11 cm from the cavity's floor. The cavity's height is 21.1 cm, placing the monopole antenna at 10 cm from the cavity's ceiling. This means the charts show the voltage levels that represent the electromagnetic field strength on a four position vertical plane cut, approximately, in the middle of the microwave oven.

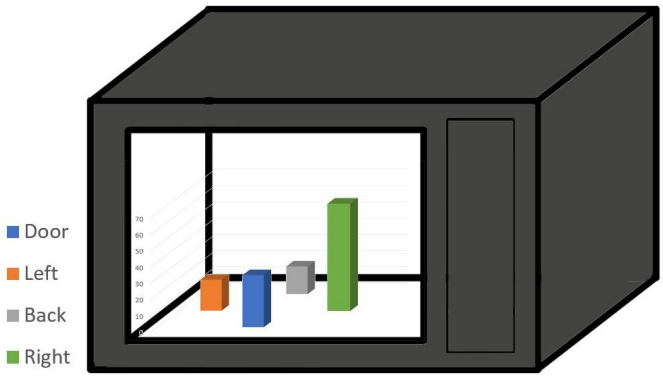

Figure 4.47: Four position test visual representation of the inductor diode-based rectifier.

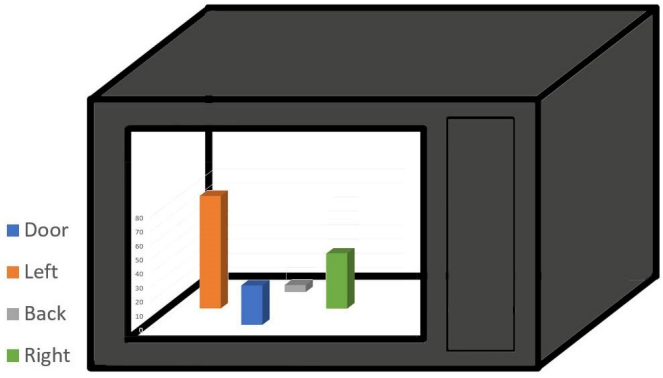

Figure 4.48: Four position test visual representation of the short stub diode-based rectifier.

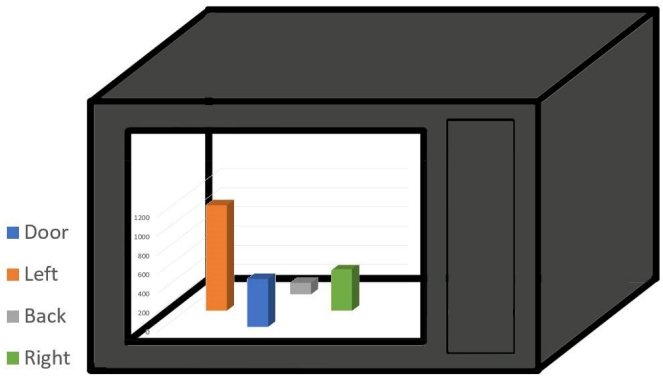

Figure 4.49: Four position test visual representation of the transistor-based rectifier.

Conclusion and Future Work

Conclusion

The microwave ovens have been in the market for 50 years and they are finally evolving with the new breakthroughs in RF engineering. The solid state technology is very promising and will most definitely revolutionise the way people cook, by introducing a new way of 'sensing' and adapting to different foods. However, even with this technology, there is still a big struggle in the development of this device, since researchers are presented with a visual handicap when it comes to the electromagnetic fields inside the microwave oven.

This dissertation proposes a way to change that by teaming up microwave theory with components unusual for this kind of application. Firstly, a study and design of electrically small antennas is presented. This type of antennas use several techniques to achieve miniaturisation of electrical size of an antenna, like bent lines, slots or metamaterial-inspired techniques. However, since the power levels are too high, a simple monopole with a rudmentary adaptation is chosen in order to deliver less power to relax the conversion stage. This stage converts the RF energy to a DC power and, unlike others of its kind, is not optimised for maximum efficiency. The goal is to have a RF to DC conversion that doesn't exceed the maximum ratings of the used components (diodes, transistors, inductors, resistors and capacitors).

After the design of this system, several other obstacles had to be taken into account. The most critical one is that, even if the converter is capable of handling very high levels of input power, the RF power radiating inside the cavity can be simultaneously captured anywhere in between the input and the output where there are microwave absorbing materials. To prevent that, an absorbing material is used together with aluminium foil to shield the RF to DC converter. The absorbent started to heat up which caused sparking in the input connector and the aluminium foil. A shielding only with the aluminium foil

(with a isolating tape on the connectors) was attempted and the testing measurements were executed with success.

The measurement probes, developed in this dissertation, serve as a proof of concept that a measurement inside the microwave oven can be done which will significantly boost the development of the new rising technologies around the microwave oven, enabling researchers to 'see' inside the cavity of this cooking appliance.

Future Work

The experiments, conducted in the scope of this dissertation, prove that components specific for this application are needed in order to optimise the monitoring probe, so that an array of probes could be placed inside the cavity to create a monitoring system with better resolution.

Other possible layouts would also be an interesting approach, like piercing holes in the cavity and sealing them with some kind of connector so that the RF to DC converters could be outside and away from high power radiation (companies produce high quantities of microwave ovens, so they wouldn't mind drilling 5 or 10 ovens for testing and developing their devices). Another possible arrangement would be using a false floor and putting the converters bellow to shield them. In this case, depending on the height of this new fake wall, the standing wave patterns inside the ovens could change and to compensate that an oven with height compensation would have to be built in order to have the same height as the cavity that were to be tested. With that said, microwave ovens vary a lot in size (height, width and length) and using a normal oven would probably be a good approximation.

Bibliography

[1] K. Parker and M. Vollmer, "Bad Food and Good Physics: The Development of Domestic Microwave Cookery", *Physics Education*, vol. 39, no. 1, pp. 82–90, 2004.

[2] G. Blonder. (2016). Science of the Microwave Oven, [Online]. Available: `http://www.genuineideas.com/ArticlesIndex/wave.html`.

[3] R. Wesson, *RF Solid State Cooking White Paper*. Ampleon, 2016.

[4] C Budd, A Hill, and G Hooper, "Experimental and Analytic Studies of the Microwave Heating of Cuboid Moist Foodstuffs", *University of Bath, UK*, 2007.

[5] M. Vollmer, "Physics of the Microwave Oven", *Physics Education*, vol. 39, no. 1, pp. 74–81, 2004.

[6] NXPsemiconductors. (2014). Solid State Cooking Oven Electronica 2014 Munich, Germany, [Online]. Available: `https://www.youtube.com/watch?v=erTEHUyoKN0`.

[7] M. Balk and S.-W. Baek, "A Multiphysics Approach to Magnetron and Microwave Oven Design", *Whitepaper of CST AG*, 2013.

[8] T Santos, L. Costa, M Valente, J Monteiro, and J Sousa, "3D Electromagnetic Field Simulation in Microwave Ovens: A Tool to Control Thermal Runaway", in *COMSOL Conference*, 2010.

[9] M Bangay and C Zombolas, "Advanced Measurements of Microwave Oven Leakage", *Radiation Protection In Australasia*, vol. 20, pp. 47–51, 2003.

[10] N. M. Zin, M. Z. M. Jenu, and F. A. Po'ad, "Measurements and Reduction of Microwave Oven Electromagnetic Leakage", in *RF and Microwave Conference (RFM), 2011 IEEE International*, IEEE, 2011, pp. 1–4.

[11] A. Mahanti, N. Carlsson, C. Williamson, and M. Arlitt, "Ambient Interference Effects in wi-fi Networks", *NETWORKING 2010*, pp. 160–173, 2010.

[12] N. Qadar, J. Khan, U. Farooq, and N. Mufti, "Investigating the Effects of Microwave Oven on the Performance of Wi-Fi Network", in *Frontiers of Information Technology (FIT), 2014 12th International Conference on*, IEEE, 2014, pp. 34–36.

[13] ANSI Standard, "Safety Level of Electromagnetic Radiation with Respect to Personnel", *ANSI C95*, vol. 1, 1966.

[14] J. Osepchuk, "A Review of Microwave Oven Safety", *Journal of Microwave Power*, vol. 13, no. 1, pp. 13–26, 1978.

[15] "Australian Standard 3301-1978 Approval and Test Specification for Particular Requirements for Microwave Ovens", *Standards Australia*,

[16] International Commission on Non-Ionizing Radiation Protection (ICNIRP), "Guidelines for Limiting Exposure to Time-Varying Electric, Magnetic, and Electromagnetic Fields (up to 300 GHz)", *Health Physics*, vol. 74, no. 4, pp. 494–521, 1998.

[17] Australian Radiation Protection and Nuclear Safety Agency (ARPANSA), "Radiation Protection Standard: Maximum Exposure Levels to Radiofrequency Fields — 3 KHz to 300 GHz", *Radiation Protection Series*, no. 3, 2002.

[18] R. F. Schiffmann and R. Steiner, "Inexpensive Microwave Leakage Detectors - Are They Worth It? (A Performance Evaluation Report)", *Journal of Microwave Power and Electromagnetic Energy*, vol. 46, no. 3, pp. 128–138, 2012.

[19] Narda Safety Test Solutions, *Narda Broadband Field Meter: NBM-520 Measuring Electric And Magnetic Fields*.

[20] C. A. Balanis, "Antenna Theory: Analysis and Design", *MICROSTRIP ANTENNAS, Third Edition, John wiley & sons*, 2005.

[21] "IEEE Standard for Definitions of Terms for Antennas", *IEEE Std 145-2013 (Revision of IEEE Std 145-1993)*, pp. 1–50, 2014. DOI: 10.1109/IEEESTD.2014.6758443.

[22] Y. Rahmat-Samii, L. I. Williams, and R. G. Yaccarino, "The UCLA Bi-polar Planar-Near-Field Antenna-Measurement and Diagnostics Range", *IEEE Antennas and Propagation Magazine*, vol. 37, no. 6, pp. 16–35, 1995.

[23] C. A. Balanis, "Antenna Theory: A review", *Proceedings of the IEEE*, vol. 80, no. 1, pp. 7–23, 1992.

[24] R. W. Ziolkowski and N. Engheta, "Metamaterial Special Issue Introduction", *IEEE Transactions on Antennas and Propagation*, vol. 51, no. 10, pp. 2546–2549, 2003.

[25] H. Wong, K.-M. Luk, C. H. Chan, Q. Xue, K. K. So, and H. W. Lai, "Small Antennas in Wireless Communications", *Proceedings of the IEEE*, vol. 100, no. 7, pp. 2109–2121, 2012.

[26] L. J. Chu, "Physical Limitations of Omni-directional Antennas", *Journal of applied physics*, vol. 19, no. 12, pp. 1163–1175, 1948.

[27] D. F. Sievenpiper, D. C. Dawson, M. M. Jacob, T. Kanar, S. Kim, J. Long, and R. G. Quarfoth, "Experimental Validation of Performance Limits and Design Guidelines for Small Antennas", *IEEE Transactions on Antennas and Propagation*, vol. 60, no. 1, pp. 8–19, 2012.

[28] H. A. Wheeler, "Fundamental Limitations of Small Antennas", *Proceedings of the IRE*, vol. 35, no. 12, pp. 1479–1484, 1947.

[29] J. Volakis, C.-C. Chen, and K. Fujimoto, *Small Antennas: Miniaturization Techniques & Applications*. McGraw Hill Professional, 2009.

[30] M. H. Rehmani, A. Rachedi, S. Lohier, T. Alves, and B. Poussot, "Intelligent Antenna Selection Decision in IEEE 802.15. 4 Wireless Sensor Networks: An Experimental Analysis", *Computers & Electrical Engineering*, vol. 40, no. 2, pp. 443–455, 2014.

[31] X. Zhang, A. Salo, and A. T. Team, "Design of Novel Wideband Planar Inverted-F Antenna for Mobile Application", in *PIERS Proceedings*, 2009, pp. 1191–1195.

[32] R. Gómez-Villanueva, R. Linares-y Miranda, J. A. Tirado-Mendez, and H. Jardón-Aguilar, "Ultra-Wideband Planar Inverted-F Antenna (PIFA) for Mobile Phone Frequencies and Ultra-Wideband Applications", *Progress In Electromagnetics Research C*, vol. 43, pp. 109–120, 2013.

[33] M. Li, Q. Xue, and W. Che, "Wideband-Integrated Planar Inverted-F Antenna with Meander Line Structures", *Microwave and optical technology letters*, vol. 51, no. 2, pp. 384–387, 2009.

[34] A. A. Salih and M. S. Sharawi, "A Dual-Band Highly Miniaturized Patch Antenna", *IEEE Antennas and Wireless Propagation Letters*, vol. 15, pp. 1783–1786, 2016.

[35] J Zhu and G. Eleftheriades, "Dual-Band Metamaterial-Inspired Small Monopole Antenna for WiFi Applications", *Electronics Letters*, vol. 45, no. 22, pp. 1104–1106, 2009.

[36] M. Selvanayagam and G. V. Eleftheriades, "A Compact Printed Antenna with an Embedded Double-Tuned Metamaterial Matching Network", *IEEE Transactions on Antennas and Propagation*, vol. 58, no. 7, pp. 2354–2361, 2010.

[37] W. C. Brown, "The History of Power Transmission by Radio Waves", *IEEE Transactions on microwave theory and techniques*, vol. 32, no. 9, pp. 1230–1242, 1984.

[38] C. R. Valenta and G. D. Durgin, "Harvesting Wireless Power: Survey of Energy-Harvester Conversion Efficiency in Far-Field, Wireless Power Transfer Systems", *IEEE Microwave Magazine*, vol. 15, no. 4, pp. 108–120, 2014.

[39] M. N. Ruiz, R. Marante, and J. A. García, "A Class E Synchronous Rectifier Based on an E-pHEMT Device for Wireless Powering Applications", in *Microwave Symposium Digest (MTT), 2012 IEEE MTT-S International*, IEEE, 2012, pp. 1–3.

[40] R. Correia and N. B. Carvalho, "HEMT Based RF to DC Converter Efficiency Enhancement Using Special Designed Waveforms", in *Microwave Symposium (IMS), 2017 IEEE MTT-S International*, IEEE, 2017, pp. 609–612.